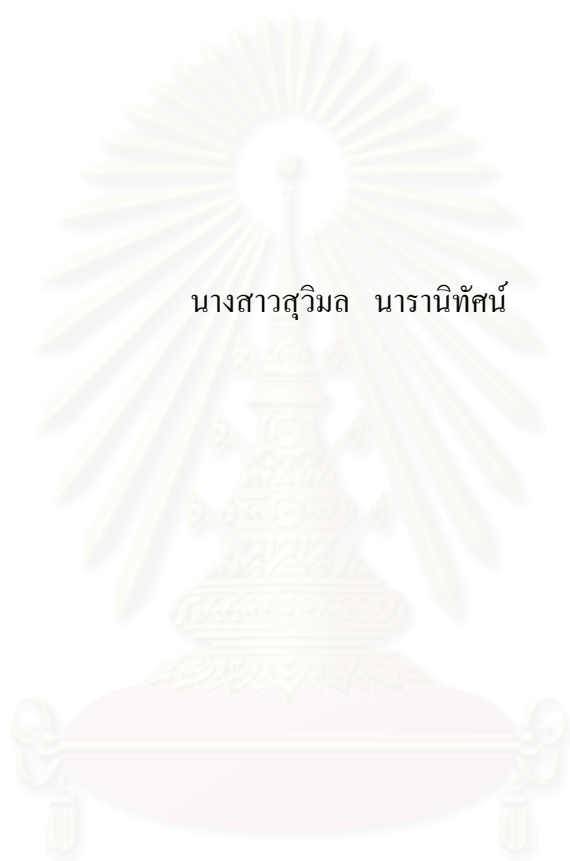


การวิเคราะห์เส้นผมด้วยเอทีอาร์เอฟทีไออาร์ไมโครสเปกโทรสโกปี



นางสาวสุวิมล นารานิต์สน์

สถาบันวิทยบริการ  
จุฬาลงกรณ์มหาวิทยาลัย

วิทยานิพนธ์นี้เป็นส่วนหนึ่งของการศึกษาตามหลักสูตรปริญญาวิทยาศาสตรมหาบัณฑิต

สาขาวิชาปิโตรเคมีและวิทยาศาสตร์พอลิเมอร์

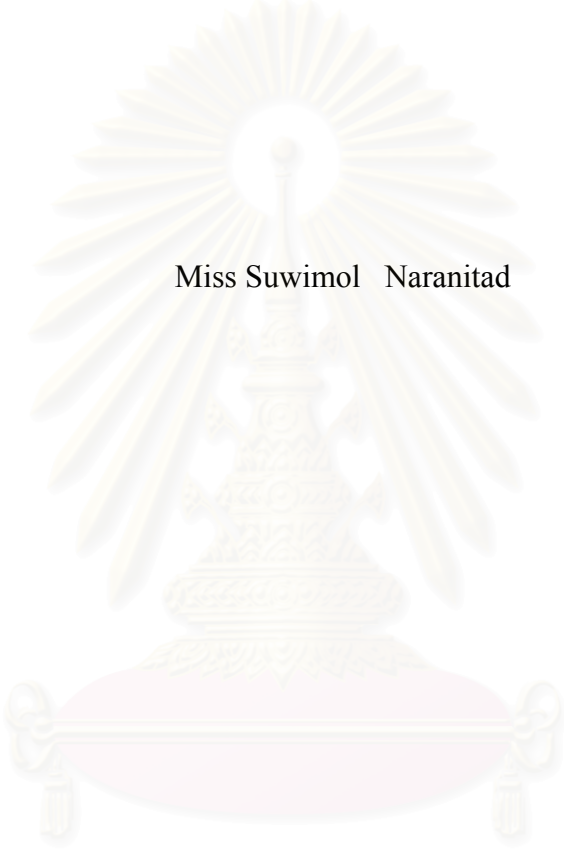
คณะวิทยาศาสตร์ จุฬาลงกรณ์มหาวิทยาลัย

ปีการศึกษา 2549

ลิขสิทธิ์ของจุฬาลงกรณ์มหาวิทยาลัย

ANALYSIS OF HUMAN HAIR BY ATR FT-IR MICROSPECTROSCOPY

Miss Suwimol Naranitad



สถาบันวิทยบริการ  
จุฬาลงกรณ์มหาวิทยาลัย

A Thesis Submitted in Partial Fulfillment of the Requirements  
for the Degree of Master of Science Program in Petrochemistry and Polymer Science

Faculty of Science

Chulalongkorn University

Academic Year 2006

Copyright of Chulalongkorn University



สุวิมล นารานีทัศน์: การวิเคราะห์เส้นผมด้วยเอทีอาร์เอฟทีไออาร์ไมโครสเปกโทรสโกปี (ANALYSIS OF HUMAN HAIR BY ATR-FT-IR MICROSPECTROSCOPY) อ. ที่ปรึกษา: รศ. ชูชาติ ธรรมเจริญ, อ. ที่ปรึกษาร่วม: รศ. ดร. สนอง เอกสิทธิ์, 67 หน้า.

อุปกรณ์เจอร์มานเนียมไมโครไออาร์อีแบบสไลด์ถูกออกแบบขึ้นมาเพื่อใช้ในการวิเคราะห์สารตัวอย่างที่มีขนาดเล็ก อุปกรณ์นี้ใช้ในการวิเคราะห์เส้นผมด้วยเทคนิคเอทีอาร์ที่ถูกนำมาใช้งานร่วมกับกล้องจุลทรรศน์อินฟราเรด เอทีอาร์สเปกตรัมที่ได้จากการวิเคราะห์ด้วยอุปกรณ์นี้มีลักษณะสเปกตรัมเหมือนกับสเปกตรัมที่ได้จากการวิเคราะห์ด้วยเทคนิคเอทีอาร์ที่ใช้กันโดยทั่วไป (ไออาร์อีรูปร่างทรงกลม) ค่าความเข้มของการดูดกลืนแสงของเส้นผมที่ได้จากการวิเคราะห์ด้วยอุปกรณ์เจอร์มานเนียมไมโครไออาร์อีแบบสไลด์จะสูงกว่าสเปกตรัมที่ได้จากเทคนิคเอทีอาร์ที่ใช้กันโดยทั่วไปเนื่องจากมีบริเวณพื้นที่สัมผัสกับสารตัวอย่างที่มีขนาดเล็กประมาณ 100x100 ตารางไมโครเมตร ทำให้สามารถวิเคราะห์สารที่มีขนาดเล็กโดยไม่ต้องมีการเตรียมตัวอย่าง การวิเคราะห์ใช้เวลาน้อยและผลการทดลองถูกต้องและเชื่อถือได้ สเปกตรัมของเส้นผมแสดงให้เห็นความแตกต่างระหว่างเส้นผมที่ไม่ผ่านการปรับปรุงและเส้นผมที่ผ่านการปรับปรุงด้วยสารเคมี เส้นผมที่ไม่แตกปลายและเส้นผมแตกปลาย และความแตกต่างของชนิดของเครื่องสำอางบริเวณพื้นผิวของเส้นผมได้ สเปกตรัมที่ได้มีความสัมพันธ์โดยตรงกับการเปลี่ยนแปลงของโมเลกุลที่เกิดขึ้นในระดับโมเลกุลของเส้นผม จากผลการทดลองสามารถนำไปประยุกต์ใช้ในการวิเคราะห์เชิงนิติวิทยาศาสตร์ได้

สถาบันวิทยบริการ  
จุฬาลงกรณ์มหาวิทยาลัย

สาขาวิชา ..... ปิโตรเคมีและวิทยาศาสตร์พอลิเมอร์ ..... ลายมือชื่อนิสิต..... สุวิมล นารานีทัศน์  
ปีการศึกษา..... 2549 ..... ลายมือชื่ออาจารย์ที่ปรึกษา.....  
ลายมือชื่ออาจารย์ที่ปรึกษาร่วม.....

# # 4872527123: MAJOR PETROCHEMISTRY AND POLYMER SCIENCE

KEYWORD: HOMEMADE SLIDE-ON Ge IRE / SINGLE HUMAN HAIR / ATR FT-IR MICROSPECTROSCOPY

SUWIMOL NARANITAD: ANALYSIS OF HUMAN HAIR BY ATR FT-IR MICROSPECTROSCOPY. THESIS ADVISOR: ASSOC. PROF. CHUCHAAT THAMMACHAROEN, CO-ADVISOR: ASSOC. PROF. SANONG EKGASIT, PH.D. 67 pp.

Homemade slide-on Ge  $\mu$ IRE accessory was designed for analysis of small amount sample. The accessory was employed for ATR FT-IR spectral acquisition of single human hair by using an infrared microscope. The spectrum acquired by the slide-on Ge  $\mu$ IRE was similar to those acquired by conventional ATR technique (Hemispherical Ge IRE). The spectral intensity of single human hair acquired by slide-on Ge  $\mu$ IRE is higher than the spectrum acquired by conventional ATR technique. Due to the small contact area of the  $\mu$ IRE is less than  $100 \times 100 \mu\text{m}^2$ , the small amount sample could be analyzed without an additional sample preparation. The analysis takes only a short time while the results are accurate and reliable. The observed spectra shows the different spectrum between untreated-hair and chemical treated-hair, un-split and split hairs, and the different type of cosmetics on hair surface. The observed spectra were directly associated with molecular changes occurring at the molecular level. The results can be applied for forensic analysis.

สถาบันวิทยบริการ  
จุฬาลงกรณ์มหาวิทยาลัย

Field of student ..Petrochemistry and Polymer Science Student's signature... *ผู้พล... ภาสารณ์*  
Academic year .....2006..... Advisor's signature... *C. Thammacharoen.*  
Co-advisor's signature... *Sanong Ekgasit*



## ACKNOWLEDGEMENTS

I would like to express my sincere gratitude to Associate Professor Dr. Sirirat Kokpol, Associate Professor Dr. Supason Wanichweacharungruang, and Associate Professor Dr. Wimonrat Trakarnpruk, for the insightful suggestions and contribution as thesis committee.

Gratefully thanks to my thesis advisor and co-advisor, Associate Professor Chuchaat Thammacharoen and Associate Professor Dr. Sanong Ekgasit, who always provides me the useful guidance, suggestion, encouragement, and understanding and also patiently practices my technical skill during the whole research.

I gratefully acknowledge the Sensor Research Unit, Department of Chemistry, Faculty of Science, Chulalongkorn University for instrumental support and Mr. Taweesak Janduang who fabricated the homemade accessory for this research. I am thankful to volunteer for the hair samples. I also would like to acknowledge Dr. Pimthong Thongnopkun for guidance, suggestion, and encouragement during my entire study.

I would like to thank my friends and colleagues at the Sensor Research Unit for the friendship and spiritual supports.

Finally, I would like to thank my wonderful parents and the endearing family for their love, understanding, encouragement, and overwhelmingly support.

# CONTENTS

	Page
ABSTRACT IN THAI.....	iv
ABSTRACT IN ENGLISH.....	v
ACKNOWLEDGEMENTS.....	vi
CONTENTS.....	vii
LIST OF FIGURES.....	xi
LIST OF TABLES.....	xv
LIST OF ABBREVIATIONS.....	xvi
LIST OF SYMBOLS.....	xvii
CHAPTER I INTRODUCTION.....	1
1.1 Human Hair.....	1
1.1.1 Human Hair Structure.....	1
1.1.2 Variation in Human Hair.....	3
1.1.2.1 Variation with Type of Human Hair.....	3
1.1.2.2 Variation with Age.....	3
1.1.2.3 Variation with Color.....	3
1.1.2.4 Variation with Amino Acid.....	4
1.1.2.5 Genetically Influences.....	5
1.1.2.6 Dietary Influences.....	5
1.1.2.7 Cosmetic Influences.....	5
1.1.2.8 Variation with Heat.....	5
1.1.2.9 Variation with Weather.....	5
1.1.2.10 Variation with Physical Wear.....	6
1.2 Hair Analysis.....	6
1.2.1 Fourier Transform Infrared (FT-IR) Spectroscopy.....	6
1.2.2 Attenuated Total Reflection Fourier Transform Infrared (ATR FT-IR) Microspectroscopy.....	7
1.3 The Objectives of This Research.....	8

	Page
1.4 The Scope of This Research.....	8
<b>CHAPTER II THEORETICAL BACKGROUND.....</b>	<b>9</b>
2.1 Biochemistry of Human Hair.....	9
2.1.1 Human Hair Growth Cycle.....	9
2.1.2 Bonding in Keratin Protein.....	9
2.1.2.1 The Hydrogen Bond.....	10
2.1.2.2 The Salt Bond.....	10
2.1.2.3 The Cystine Bond.....	10
2.1.2.4 The Sugar Bond.....	10
2.2 ATR FT-IR Spectroscopy.....	11
2.2.1 Principles of Light Reflection and Refraction.....	12
2.2.2 Internal Reflection Element (IRE).....	14
2.2.3 ATR Spectral Intensity and Depth of Penetration.....	15
2.2.4 Problem of Single Fiber in Conventional ATR Accessory.....	19
2.3 ATR FT-IR Microspectroscopy.....	20
2.3.1 Infrared Microscope.....	20
2.3.2 Homemade Slide-on Ge $\mu$ IRE Accessory.....	21
2.3.2.1 Ray Tracing of Homemade Slide-on Ge $\mu$ IRE.....	22
<b>CHAPTER III EXPERIMENTAL SECTION.....</b>	<b>24</b>
3.1 Materials and Equipments .....	24
3.1.1 Sample.....	24
3.1.2 Instruments .....	24
3.2 Default Spectral Acquisition.....	25
3.3 The Homemade Slide-on Ge $\mu$ IRE Accessory.....	25
3.4 Characterization of Single Human Hair by ATR FT-IR Spectroscopy	27
3.4.1 Experimental Procedure for the Conventional ATR Accessory...	27
3.4.2 Experimental Procedure for the Homemade Slide-on Ge $\mu$ IRE Accessory .....	28



	Page
3.5 Characterization of Trace Cosmetic on the Hair Surface by ATR FT-IR Spectroscopy.....	30
3.5.1 Experimental Procedure for the Conventional ATR Accessory..	30
3.5.2 Experimental Procedure for the Homemade Slide-on Ge $\mu$ IRE Accessory.....	31
3.6 Characterization of Split Hairs by ATR FT-IR Microspectroscopy....	32
3.6.1 Experimental Procedure for the Homemade Slide-on Ge $\mu$ IRE Accessory.....	32
 CHAPTER IV RESULTS AND DISCUSSION.....	 34
4.1 Efficiency of Homemade Slide-on Ge $\mu$ IRE Accessory .....	34
4.2 Chemical Information of Human Hair.....	36
4.3 Characterization of Single Human Hair by ATR FT-IR Microspectroscopy .....	37
4.3.1 Untreated-Hair.....	38
4.3.1.1 ATR FT-IR Spectra of Hairs from Different Persons with Different Ages.....	38
4.3.1.2 ATR FT-IR Spectra of Hairs from Male and Female.....	38
4.3.1.3 ATR FT-IR Spectra of hairs from the Individual Person with Different Natural Hair Color.....	41
4.3.1.4 ATR FT-IR Spectra of Hairs from Different Position along the Hair Filament and Different Position of Hair on Head.....	43
4.3.1.5 ATR FT-IR Spectra of Hairs from Different Persons.....	46
4.3.2 Chemical Treated-Hair .....	47
4.3.2.1 Comparison of ATR FT-IR Spectra of Hairs between Untreated-Hair and Straight Creams Treated-Hair.....	48

	Page
4.3.2.2 Comparison of ATR FT-IR Spectra of Hairs between Untreated-Hair and Permanent Wave Lotion Treated-Hair.....	49
4.2.2.3 Comparison of ATR FT-IR Spectra of Hairs between Untreated-Hair and Color Cream Treated-Hair.....	50
4.4 Characterization of Trace Cosmetic on the Hairs Surface by using ATR FT-IR Spectroscopy.....	51
4.4.1 Conventional ATR Technique.....	52
4.4.2 Homemade Slide-on Ge $\mu$ ATR Technique.....	53
4.4.2.1 Results of the Different Type of Cosmetics.....	54
4.5 Characterization of Split Hairs by ATR FT-IR Microspectroscopy....	57
CHAPTER V CONCLUSIONS.....	60
REFERENCES.....	62
CURRICULUM VITAE.....	67

สถาบันวิทยบริการ  
จุฬาลงกรณ์มหาวิทยาลัย

## LIST OF FIGURES

Figure	Page
1.1 Backbone structure of human hair protein.....	1
1.2 Alpha helix structure of human hair.....	2
1.3 Human hair structures.....	2
2.1 The four types of bonding of keratin proteins in human hair .....	11
2.2 Schematic diagram of the radiation propagates through the internal reflection element (IRE).....	12
2.3 Reflection and refraction of a plane wave at a dielectric based on Snell's Law.....	13
2.4 Condition under which total internal reflection occurs. Light travels from an optically denser medium and impinges at the surface of the optically rarer medium ( $n_1 > n_2$ ) with angle of incidence equal the critical angle.....	14
2.5 Selected IRE configurations commonly used in ATR experimental setups: (a) Single reflection variable-angle hemispherical crystal and (b) Multiple reflection single-pass crystal.....	14
2.6 Depth dependence MSEvF at various frequencies with (A) p-polarized radiation and (B) s-polarized radiation. The simulation parameter are $n_0 = 4.0$ , $n_1 = 1.5$ , $k_1 = 0.0$ , $\theta = 45^\circ$ , and $\nu = 500, 1000, 1500$ , and $3000 \text{ cm}^{-1}$ .....	18
2.7 Depth dependence MSEvF at various angles of incidence with (A) p-polarized radiation and (B) s-polarized radiation. The simulation parameter are $n_0 = 4.0$ , $n_1 = 1.5$ , $k_1 = 0.0$ , $\nu = 1000 \text{ cm}^{-1}$ , and $\theta = 30^\circ, 35^\circ, 40^\circ, 45^\circ, 50^\circ, 55^\circ$ , and $60^\circ$ .....	19
2.8 An optical diagram of an infrared microscope.....	21
2.9 A Schematic illustration of ray tracing within the 15 X Schwarzschild Cassegrain infrared objective.....	22

Figure	Page
3.1 The homemade slide-on Ge $\mu$ IRE accessory was developed by Sensor Research Unit, Department of chemistry, Faculty of Science, Chulalongkorn University, Bangkok 10330, Thailand.....	26
3.2 The homemade slide-on Ge $\mu$ IRE accessory mounted onto the infrared microscope.....	27
3.3 Experimental procedures for ensuring the optical contact between a sample and the IRE of the conventional ATR accessory.....	28
3.4 Experimental procedures for ensuring the optical contact between a sample and the IRE of the homemade slide-on Ge $\mu$ IRE accessory.....	29
3.5 The sampling positions along the single human hair in the first experiment.....	29
3.6 Single human hair from various positions on a head were analyzed in the second experiment.....	30
3.7 Experimental procedures for spectral acquisition using <i>Contact-and-Collect</i> technique by the hemispherical Ge IRE: (A) the hair sample was raised until the hair touched the IRE with applied pressure, (B) the hair sample was contacted the IRE and characterized the cosmetics and hair, and (C) the hair sample was removed from the IRE and characterized the cosmetic without interference of hair.....	31
3.8 Experimental procedure for spectral acquisition using <i>Contact-and-Collect</i> technique by the homemade slide-on Ge $\mu$ IRE accessory: (A) the hair sample was raised until the hair touched the IRE with applied pressure, (B) the hair sample was contacted the IRE and characterized the cosmetics and hair, and (C) the hair sample was removed from the IRE and characterized the cosmetic without interference of hair.....	32
3.9 The sampling positions of split hairs by the homemade slide-on Ge $\mu$ IRE accessory.....	33
4.1 ATR FT-IR spectra of single human hair acquired by: (A) Conventional Ge IRE and (B) Homemade slide-on Ge $\mu$ IRE accessories.....	35

Figure	Page
4.2 Normalized ATR FT-IR spectra of single hair from a person at three positions. The insert were normalized spectra by Amide I absorption band ( $1637\text{ cm}^{-1}$ ).....	35
4.3 ATR FT-IR spectrum of single hair.....	36
4.4 ATR FT-IR spectra of human hair from different persons.....	40
4.5 ATR FT-IR spectra of single human hair from persons with different gender: (A) males and (B) females.....	41
4.6 ATR FT-IR spectra of hair from individual person with different natural hair color.....	42
4.7 The sampling positions along the single human hair.....	43
4.8 Normalized ATR FT-IR spectra of hair were collected along the hair filament.....	44
4.9 Positions on individual person when hair samples were collected.....	45
4.10 Normalized spectra of hair acquired from the different positions of hair on head.....	45
4.11 Normalized spectra of single hair from eight persons .....	46
4.12 ATR FT-IR spectra of treated single hair with different type of chemical treatment.....	47
4.13 ATR FT-IR spectra of hair (a) untreated-hair and (b) treated-hair with straight cream.....	49
4.14 ATR FT-IR spectra of hair (a) untreated-hair and (b) treated-hair with permanent wavy lotion.....	50
4.15 ATR FT-IR spectra of hair (a) untreated-hair and (b) treated-hair with color cream.....	51
4.16 ATR FT-IR spectra of hair and residual cosmetics on IRE (A) clean-hair and (B) uncleaned-hair acquired by the conventional ATR technique.....	53
4.17 ATR FT-IR spectra of hair and residual cosmetics on IRE (A) clean-hair and (B) uncleaned-hair acquired by the homemade slide-on Ge $\mu$ IRE accessory.....	55



Figure	Page
4.18 ATR FT-IR spectra of hair and residual cosmetics on IRE: (A) hair and (B) residual cosmetics acquired by the homemade slide-on Ge $\mu$ IRE accessory.....	56
4.19 ATR FT-IR spectra of split hairs and un-split hairs acquired by the homemade slide-on Ge $\mu$ IRE accessory.....	57
4.20 ATR FT-IR spectra of hair acquired by the homemade slide-on Ge $\mu$ IRE: (A) un-split hairs, (B) split hairs, and (C) making-split hairs.....	58



สถาบันวิทยบริการ  
จุฬาลงกรณ์มหาวิทยาลัย

## LIST OF TABLES

Table	Page
1.1 Amino acid content of human hair .....	4
4.1 Peak assignments of human hair .....	37



สถาบันวิทยบริการ  
จุฬาลงกรณ์มหาวิทยาลัย

## LIST OF ABBREVIATIONS

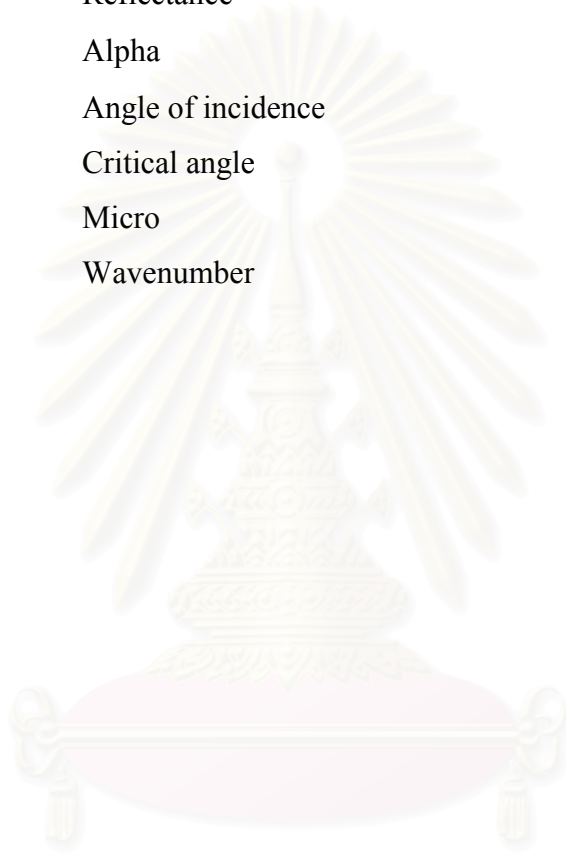
ATR	Attenuated total internal reflection
DNA	Deoxyribonucleic acid
FT-IR	Fourier transform infrared spectroscopy
Ge	Germanium
ICP	Inductively coupled plasma
IRE	Internal reflection element
KBr	Potassium bromide
MCT	Mercury-cadmium-telluride
MSEF	Mean square electric field
MSEvF	Mean square evanescent field
SNR	Signal-to-noise-ratio
ToF-SIMS	Time-of-flight secondary ion mass spectrometers



สถาบันวิทยบริการ  
จุฬาลงกรณ์มหาวิทยาลัย

## LIST OF SYMBOLS

$A$	Absorbance
$d_p$	Penetration depth
$I$	Intensity
$n$	Refractive index
$R$	Reflectance
$\alpha$	Alpha
$\theta$	Angle of incidence
$\theta_c$	Critical angle
$\mu$	Micro
$\nu$	Wavenumber



สถาบันวิทยบริการ  
จุฬาลงกรณ์มหาวิทยาลัย

# CHAPTER I

## INTRODUCTION

Hair is natural polymers, which have keratin fibers composition. Different type of hair is depending on the race and genetic of person. Hair damage occurs from life style, hair treatment, diet, and health of person. Thus, difference of hair can be identified the hair from individual person.

### 1.1 Human Hair

#### 1.1.1 Human Hair Structure

Human hair composed primarily of proteins. These proteins are strong structure protein and hard fibrous type called keratin, which composed of many amino acids linked by peptide bond called “polypeptide”. The backbone structure of polypeptide in protein structure of human hair is shown in Figure 1.1.

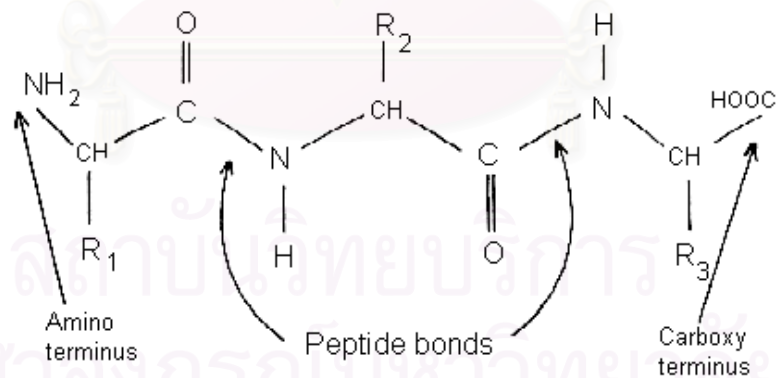


**Figure 1.1** Backbone structure of human hair protein.

The alpha helix structure occurs from the polypeptide chains that forms the keratin protein found in human hair as shown in Figure 1.2. In the organization of a single human hair, three alpha helices are twisted together to form a “*protofibril*”. Nine protofibrils are then bundled in a circle to form an eleven-stranded cable known



as the “*microfibril*”. These microfibrils are joined together to form a “*macrofibril*” and these microfibrils are found in cortex layers of hair.

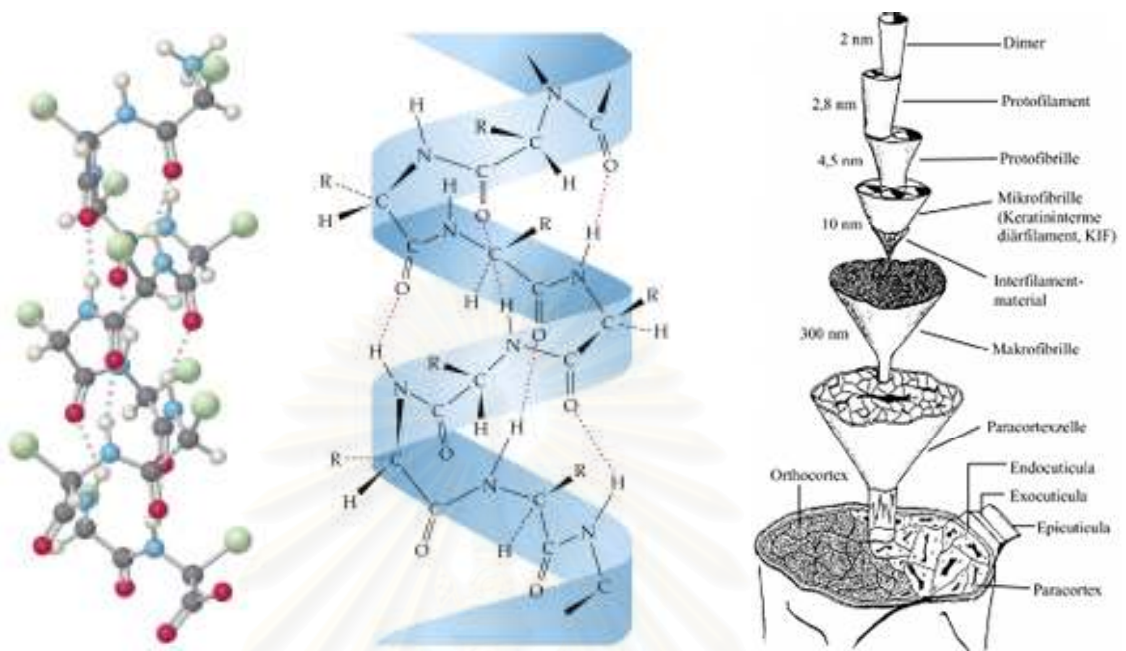


**Figure 1.2** Alpha helix structure of human hair.

The human hair consists of three layers in each single hair fiber. The innermost layer or *medulla* is the large layer of hairs. The second or middle layer known as the *cortex* provided strength, color, and texture of hair. Finally, the outermost layer or *cuticle* is thin layer, colorless, and can be protector of the hair. Human hair structures were shown in Figure 1.3.

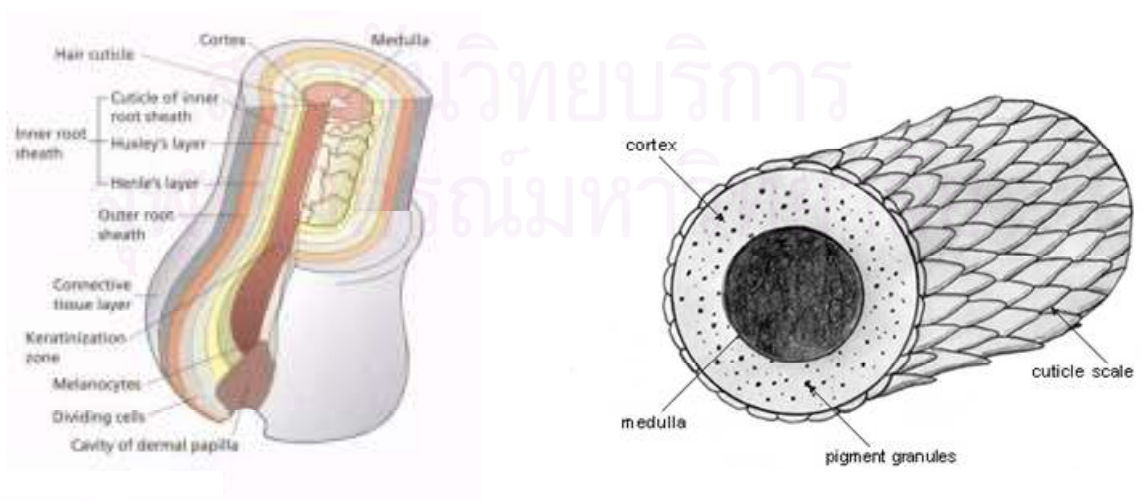


**Figure 1.3** Human hair structures.

## 1.1.2 Variation in Human Hair

Different people have different hair depending on physical property (i.e., color, length, diameter, and amino distribution), race, genetic, hair treatment, dietary, and healthy. These factors are influenced on human hair structure.

### 1.1.2.1 Variation with Type of Human Hair

Three types of hair growth on the human including:

**Lanugo hairs** are the hairs that develop on an unborn baby. The period of growth has about three months. The hairs are fine and soft, and contain no pigment.

**Vellus hairs** are short hairs, which having length of 2.5 centimeter and contain little or no pigment.

**Terminal hairs** are the long hairs that growth on the head and in many people on the body, arms, and legs. The hairs are changed by factors of hair damage.

### 1.1.2.2 Variation with Age

Age has no influence on chemical structure of hair. But the times of life are affected by natural factors including metabolism, diet, hair damage, race, hormone, and age [36].

### 1.1.2.3 Variation with Color

The occurrence of the color of hair comes from the presence of pigment in cortex layer of human hair. The pigment cells called “melanin” created a black pigment. The different hair colors are relative to amounts of melanin [37, 38].

#### 1.1.2.4 Variation with Amino Acids

The human hair is composed of many amino acids, which has different quantity, ratio, and distribution. The amino acid contents of hairs are shown in Table 1.1 [1, 39].

**Table 1.1** Amino acid contents of human hair [1]

Amino acid	% <sup>d</sup>
Alanine	6.9
Arginine	7.2
Aspartic acid <sup>a</sup>	9.3
Half cystine <sup>b</sup>	7.6
Glutamic acid <sup>c</sup>	16.6
Glycine	5.2
Histidine	0.7
Isoleucine	3.7
Leucine	10.2
Lysine	3.5
Methionine	0.4
Phenylalanine	2.0
Proline	3.8
Serine	9.0
Threonine	5.5
Tyrosine	2.5
Valine	6.1

<sup>a</sup> Includes asparagines.

<sup>b</sup> Cysteine plus half cystine.

<sup>c</sup> Includes glutamine.

<sup>d</sup> Measured as residue per 100 amino acid residues.

#### **1.1.2.5 Genetically Influences**

From the various amino contents in human hair, the genetic is one of influences of different hairs. The several human hairs were followed by the determination of the amino acid in hair. The higher levels of cystine in hairs from male are more than that of female [39, 40].

#### **1.1.2.6 Dietary Influences**

The amino acid contents of human hair (i.e., cystine, arginine, and methionine) in individual persons have contained the different sulfur suffering from diet. The diet has an influence on amino acid content in human hair, which decreased or increased the synthesis of sulfur proteins.

#### **1.1.2.7 Cosmetic Influences**

Hair treatment includes hair coloring, permanent waving, straightening, and bleaching. These treatments used strong chemicals applied directly to the hairs and are affected the protein structure in hair because they destroyed the cuticle layer. The damage of hair can be occurred by breaking of protein bond in cortex layer.

#### **1.1.2.8 Variation with Heat**

The damage of hair by heat can occur from blow dryers, hot rollers, curling and straightening tool. The heat can crack the cuticle layer and evaporate water in hair which is the cause of hair damage.

#### **1.1.2.9 Variation with Weather**

Ultraviolet ray is the cause of hair damage because the ultraviolet can break protein bond in hair. The chemical structure of hair is changed in molecular level.

### **1.1.2.10 Variation with Physical Wear**

The damage of hair occurred from abrasion from rough brush or comb, rubber bands, barrettes, and other accessories used of hair.

As described in the variation of human hair, the hair structure may use for identifying the hair of individual person because the different type of hair depends on the race and genetic person. However, variation of hair occurs from life style, hair treatment, diet, and health of person may be identified. Hair analysis by scientific instruments was developed, and has been applied to the biological analysis, and forensic analysis.

## **1.2 Hair Analysis**

Traditionally, analysis of human hair and/or analysis of hair surface were performed by using many techniques such as high performance liquid chromatography (HPLC) [2-5], gas chromatography/mass spectroscopy (GC/MS) [6-11], inductively coupled plasma/mass spectroscopy (ICP/MS) [12], time-of-flight secondary ion mass spectroscopy (ToF-SIMS) [13-14], Raman spectroscopy [15], and DNA analysis [16-17]. These techniques require destructive sample analysis, an additional sample preparation, and long analysis time in order to obtain good spectral quality. Over the years, the importance of hair analysis has been demonstrated such as forensic science [18-20], environmental exposure [21-22], biological and medical science [23-27], and cosmetic science [28-30].

### **1.2.1 Fourier Transform Infrared (FT-IR) Spectroscopy**

Fourier transform infrared (FT-IR) spectroscopy is a technique based on the determination of absorption of infrared light due to energy resonance with vibrational motions of functional molecular groups [31]. This technique has been applied as an analytical technique in different fields such as geology, material science, polymer science, and many others.



Recently, FT-IR spectroscopy is the suitable technique for hair analysis. It has been suggested that infrared spectroscopy is one of the powerful technique for the forensic analysis of human hair [32]. This is due to the fact that it can provide rapid and specific chemical information at the molecular level associated with the nature of human hair and its composition. FT-IR spectroscopy is sensitive to the presences of chemical functional groups in a hair sample.

Traditionally FT-IR sampling technique is the transmission techniques using KBr pellets [33]. This is probably the most popular way of obtaining infrared spectra (i.e., by passing infrared beam directly through the sample). Since hair sample was dark color, it is one of limitation of transmission technique. The thickness is another problem in analysis. The sample thicker than 20 microns cannot analyze. Reflectance sampling techniques differ from transmission techniques in that the infrared beam is bounced off the sample instead of passing through the sample. The techniques require smooth sample in order for the sample to reflect of infrared beam. In the conventional ATR technique, requires contact between the sample and internal element (IRE) [34]. Limitations of the analysis by these techniques include the destructive sample, complicated sample preparation, large amounts of sample area for analysis, and long scanning analysis times in order to obtain good spectra. From the limitations of traditional IR technique, the FT-IR instrument and microscope attachment was developed.

### **1.2.2 Attenuated Total Reflection Fourier Transform Infrared (ATR FT-IR) Microspectroscopy**

Attenuated total reflection (ATR) technique is the surface sensitive technique. This technique involves the collection of radiation reflected from the interface between hair sample and IRE, in which the *evanescent wave* penetrated from the IRE into the hair sample. This method may solve problems associated with transmission infrared spectroscopy such as path length and concentration. Furthermore, the development of micro-sampling accessories became an essential tool in the micro-destructive analysis of small sample. Fourier transform infrared (FT-IR) microspectroscopy combines IR spectroscopy and microscopy for determining the chemical composition in small sample areas. ATR FT-IR microscope provides the

short analysis time, non-destructive sample, without additional sample preparation, and minimal sample area for analysis.

### **1.3 The Objective of This Research**

The objective of this research is to develop sampling technique and to apply the homemade slide-on Ge  $\mu$ IRE accessory for characterization of single human hair.

### **1.4 The Scope of This Research**

1. To compare ATR FT-IR spectra observed by the homemade slide-on Ge  $\mu$ IRE accessory and the conventional Ge IRE accessory.
2. To characterize a single human hair by homemade slide-on Ge  $\mu$ IRE accessory.
3. To differentiate between untreated-hair and chemical treated-hair; un-split hairs and split hairs.
4. To develop the novel sampling technique for analysis of trace and/or thin film on surface.

สถาบันวิทยบริการ  
จุฬาลงกรณ์มหาวิทยาลัย

## CHAPTER II

### THEORETICAL BACKGROUND

#### 2.1 Biochemistry of Human Hair

Human hair is natural polymer which mainly composes of the keratin protein. The hair shows the different property including the physical property and chemical property. The physical properties of hair (i.e., straight, curly, and wavy hair) occur by the growth cycle. The change of chemical bonding in human hair is affected the chemical property of hair.

##### 2.1.1 Human Hair Growth Cycle

Hair grows from a follicle. Each hair follicle has come on repeating cycle of activity. One cycle composed of three phases as follows:

**Anagen:** It is the period of active growth.

**Catagen:** It is the period of breakdown and change.

**Telogen:** It is the period of resting hair before new hair is growth and comes to repeat cycle.

##### 2.1.2 Bonding in Keratin Protein

The keratin proteins compose of amino acids, two amino acids are linked by peptide bond called “polypeptide” and the polypeptide form alpha helix structure. The alpha helix has building into protofibrils, microfibrils, macrofibrils, and then cortex layers. The hair structure occurs from the chemical bonding of amino acid in human hair. The bonds in the hair are located within each and every alpha helix. The number of amino acid in human hair has a specific character of protein.

### **2.1.2.1 The Hydrogen Bond**

The hydrogen bond in keratin protein is located between the coils of alpha helix. This bond is responsible for strength and elasticity of human hair. The temperature directory to the hair can be changed this bonds.

### **2.1.2.2 The Salt Bond**

The salt bond is an ionic bond formed by the electron transfer from the side chain of a basic amino group (an amino acid with a  $\text{COO}^-$  group) to the side chain of an acidic amino acid, i.e.  $\text{NH}_3^+$ . The salt bond is responsible for strength and elasticity of hair. This occurs in a position paralleled to the axis line of the alpha helix of the hair.

### **2.1.2.3 The Cystine Bond**

The cystine bond or disulfide bond or sulfur bond occurs by cross-linking between cystine residues (amino acids) of human hair. This bond is perpendicular to the axis of alpha helix in hair. One cystine bond occurs every four turns of the alpha helix. This position of bond is responsible for toughness of hair and sensitive responsible for chemical treatment.

### **2.1.2.4 The Sugar Bond**

The sugar bond is formed between the side chain of an amino acid having an OH group (i.e., serine, tyrosine) and an acidic amino group. This bond is formed perpendicular to the axis of the hair. It is responsible to toughness and strength in hair. The sugar bonds are affecting to the moisture content of hair.

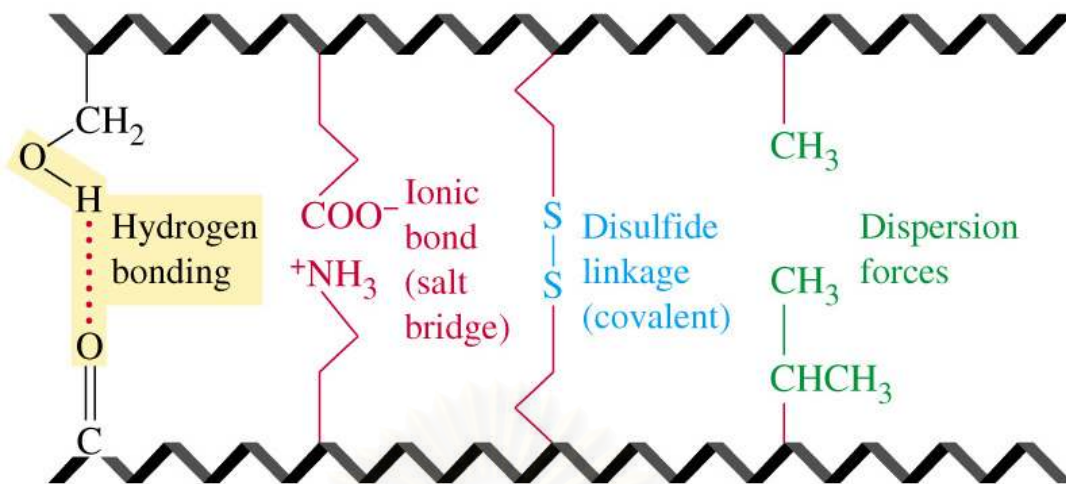


**Figure 2.1** The four types of bonding of keratin proteins in human hair.

## 2.2 ATR FT-IR Spectroscopy

Attenuated total reflection (ATR) is a surface sensitive technique. This technique is used to collect the spectra of solids, liquids, semisolids, and thin films. ATR is performed by using an accessory that mounts in the sample compartment of an FT-IR spectrometer. All the analysis required is the aligning of an ATR attachment, pressing the sample against an ATR crystal, and collecting spectra. ATR data have often been subjected to Beer-Lambert law analysis [31, 41].

$$I / I_0 = e^{-A(\nu)} = e^{-c_2 \varepsilon(\nu) l} \quad (2.1)$$

where  $A(\nu)$  is the sample absorbance at a given wavenumber  $\nu$ ,  $c_2$  is the concentration of the absorbing functional group of a sample,  $\varepsilon(\nu)$  is the wavenumber dependent extinction coefficient, and  $l$  is the film thickness for the IR beam at a normal incidence to the sample surface.

In ATR configuration, the denser medium (an internal reflection element, IRE) is in optical contact with rarer medium (a sample). The IRE is infrared transparent. The sample, on the other hand, is infrared absorbing and has a complex refractive index at frequency  $\nu$  of  $\hat{n}_1(\nu) = n_1(\nu) + ik_1(\nu)$ , where  $n_1(\nu)$  and  $k_1(\nu)$  are refractive index and absorption index, respectively. Incident light travels from the IRE and



impinges the IRE-absorbing medium interface with an angle of incidence is greater than the critical angle, total internal reflection can be occurred. The critical angle can be calculated from the refractive indices of the denser medium and the rarer medium by the following expression [41]:

$$\theta_c = \sin^{-1}(n_1 / n_0) \quad (2.2)$$

where  $n_1$  and  $n_2$  are refractive indices of denser medium and rarer medium, respectively.

### 2.2.1 Principles of Light Reflection and Refraction

Reflection of light or radiant energy is the abruptly change in the direction of propagation when the radiation is incident on an interface. An optical interface is created whenever there is a discrete change in optical properties; namely the refractive index and/or absorption index. The basic features of the propagating and evanescent fields are described in Figure 2.2 [42].

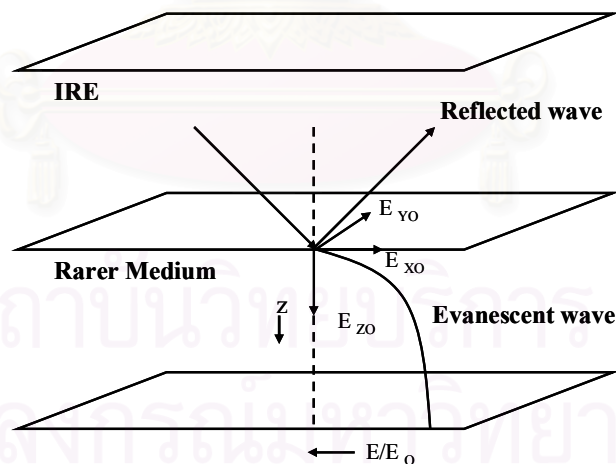


**Figure 2.2** Schematic diagram of the radiation propagates through the internal reflection element (IRE).

The electromagnetic radiation passes from one medium to another that has a different optical constant, a suddenly change of the beam direction is detected because of the differences in propagation velocity through two media. If light propagates

through a medium with refractive index  $n_1$  and enter a medium with refractive index  $n_2$  (Figure 2.3), the light path will change, and the extent of refraction is given by the following relationship [41]:

$$\frac{\sin \alpha_1}{\sin \alpha_2} = \frac{n_2}{n_1} \quad (2.3)$$

where  $\alpha_1$  and  $\alpha_2$  are the angle of incidence and refraction, respectively. When electromagnetic radiation strikes an interface between media 1 and 2 that have different refractive indices, reflection also occurs.

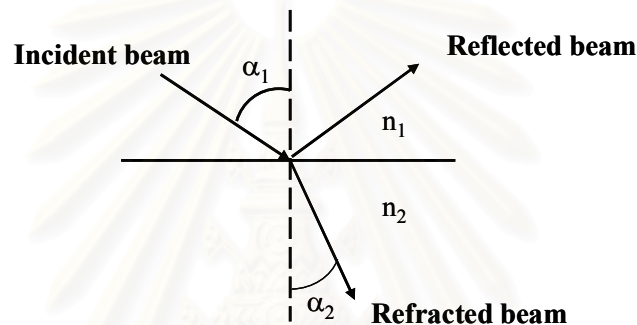


**Figure 2.3** Reflection and refraction of a plane wave at a dielectric based on Snell's Law.

Snell's law is an important phenomenon in numerous applications involving total internal reflection. Total internal reflection occurs when light traveling in an optically dense medium (one having a high refractive index) impinges on an interface with a less dense medium. As illustrated in Figure 2.4, when the angle of incidence  $\alpha_1$  equals the critical angle  $\theta_c$ ,  $\alpha_2 = 90^\circ$ .

Total internal reflection spectroscopy is, therefore, the technique of recording the optical spectrum of a sample material that is in contact with an optically denser medium. The wavelength dependence of the reflectivity of this interface is measured by introducing light into the denser medium. In this technique the reflectivity is a measure of the interaction of the electric field with the material and the resulting spectrum is also the characteristic of the material.

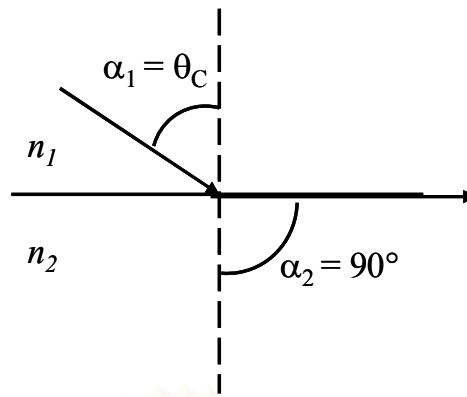


**Figure 2.4** Condition under which total internal reflection occurs. Light travels from an optically denser medium and impinges at the surface of the optically rarer medium ( $n_1 > n_2$ ) with angle of incidence equals the critical angle.

### 2.2.2 Internal Reflection Element (IRE)

The internal reflection element (IRE) is a material of high refractive index that carries the radiation to the sample in internal reflection and attenuated total reflection measurement. The IRE is transparent throughout the mid-infrared spectral region. The IRE must also withstand physical and chemical contact with samples. It is not too surprising that few materials meet these requirements. Generally speaking, the IRE configuration included variable-angle hemispherical crystal with single reflection and multiple reflection planar crystal [31]. The IRE is used in internal reflection spectroscopy for establishing the conditions necessary to obtain internal reflection spectra of materials (Figure 2.5).



(a) Single Reflection

(b) Multiple Reflection

**Figure 2.5** Selected IRE configurations commonly used in ATR experimental setups: (a) Single reflection variable-angle hemispherical crystal and (b) Multiple reflection single-pass crystal [42].

Radiation propagates through the IRE by means of internal reflection. The sample material is placed into an optical contact with the IRE. The ease of obtaining an internal reflection spectrum and the information obtained from the spectrum are determined by the characteristics of the IRE (i.e., single or multiple reflections). A choice must be made in the working angle or range of angles of incidence, number of reflections, aperture, number of passes, surface preparation, and material from which it is made [43].

### 2.2.3 ATR Spectral Intensity and Depth of Penetration

In ATR experiment, the magnitudes of the interaction between light and the sample can be expressed in terms of absorbance. The absorbance depends on both properties of material (e.g., refractive index of the IRE and complex refractive index of the sample) and the experimental parameters (e.g., angle of incidence and polarization of the incident beam). The relationship between absorbed and reflected intensity in an ATR spectrum is given by [44]:

$$A_l(\theta, \nu) = 1 - R_l(\theta, \nu) \quad (2.4)$$

where  $\theta$  is the angle of incidence,  $l$  is the degree of polarization,  $A(\theta, \nu)$  and  $R(\theta, \nu)$  are absorptance and reflectance, respectively. The polarization direction is given with respect to the plane of incidence. The plane of incidence is defined as the plane that contains both incident and reflected beam. For  $p$ -polarization ( $p$ - stands for parallel), the electric component of the electromagnetic wave is parallel to the plane of incidence while the magnetic component is perpendicular to the plane of incidence. The electric component of the electromagnetic wave with  $s$ -polarization ( $s$ - stands for senkrecht) is perpendicular to the plane of incidence while the magnetic component is parallel to the plane of incidence. In general, absorptance in ATR can be expressed in terms of experimental parameters and material characteristic by the following expression [44]:

$$A_p(\theta, \nu) = \frac{4\pi\nu}{n_0 \cos \theta} \int_0^\infty n_1(\nu) k_1(\nu) \langle E_z^2(\theta, \nu) \rangle dz \quad (2.5)$$

where  $\bar{p}$  indicates degree of polarization of the incident beam,  $\langle E_z^2(\theta, \nu) \rangle$  is the *mean square electric field* (MSEF) at depth  $z$ .  $n_1(\nu)$ , and  $k_1(\nu)$ , respectively, are the refractive index and absorption index of the sample, and  $n_0$  is the refractive index of the IRE. The MSEF has the strongest in magnitude at the IRE/sample interface. Its strength decreases exponentially as a function of depth. The MSEF is, however, also a function of experimental condition and material characteristics.

Under the ATR condition, although there is no light traveling across the IRE/sample interface, there is an evanescent field generated at the boundary. This field is strongest at the interface and exponentially decays as a function of distance from the interface. The rapid decay of the evanescent field is the unique characteristic of technique that makes ATR a powerful surface characterization technique. The decay pattern of the evanescent field can be expressed in terms of the distance from IRE/sample interface by the following expression:

$$\langle E_z^2(\theta, \nu) \rangle = \langle E_0^2(\theta, \nu) \rangle e^{-2z/d_p(\theta, \nu)} \quad (2.6)$$

where  $d_p(\theta, \nu)$  is the penetration depth.  $\langle E_0^2(\theta, \nu) \rangle$  and  $\langle E_z^2(\theta, \nu) \rangle$  are the MSEvF at the interface and the depth  $z$ , respectively.

Under a non-absorbing condition (*i.e.*,  $k_1(\nu) = 0$ ), the MSEF can be calculated if the refractive index of material is known. Under this condition, the MSEF is given a special name as the *mean square evanescent field* (MSEvF). The strength and the decay characteristic of the MSEvF can be given in a much simpler than those of MSEF. The MSEvF at the interface with  $p$ - and  $s$ -polarized radiation are given, respectively, by:

$$\langle E_{p,z=0}^2(\theta, \nu) \rangle_{k=0} = \frac{4 \cos^2 \theta [\sin^2 \theta - (n_1(\nu)/n_0)^2] + 4 \cos^2 \theta \sin^2 \theta}{[1 - (n_1(\nu)/n_0)^2] \{ [1 + (n_1(\nu)/n_0)^2] \sin^2 \theta - (n_1(\nu)/n_0)^2 \}}$$

$$\langle E_{s,z=0}^2(\theta, \nu) \rangle_{k=0} = \frac{4 \cos^2 \theta}{1 - (n_1(\nu)/n_0)^2} \quad (2.7)$$

The depth of penetration ( $d_p$ ) is defined as the depth where the electric field strength decays to 1/e of its value at the interface. The depth of penetration is given by the following equation [45]:

$$d_p = \frac{1}{2\pi\nu n_0 (\sin^2 \theta - (n_1/n_0)^2)^{1/2}} \quad (2.8)$$

where  $\nu$  is the frequency of the infrared radiation and  $\theta$  is the angle of incidence.

Equation 2.8 is complicated, but there are a few simple things about it that should be remembered. Firstly, the depth of penetration ( $d_p$ ) is dependent on wavenumber. The  $d_p$  goes down as wavenumber goes up. Thus, low wavenumber light penetrates further into the sample than high wavenumber light. The evanescent field also varies as a function of frequency of the radiation. The depth-dependent MSEvFs at various frequencies are shown in Figure 2.6. If the refractive indices at two different frequencies are the same, their MSEvFs at the interface are the same. However, their decay characteristics are different. The greater the frequency, the faster the decay of the field. As a result, the evanescent field at a greater frequency decays to zero at a shallower depth than that of at a lower frequency.

สถาบันวิทยบริการ  
จุฬาลงกรณ์มหาวิทยาลัย



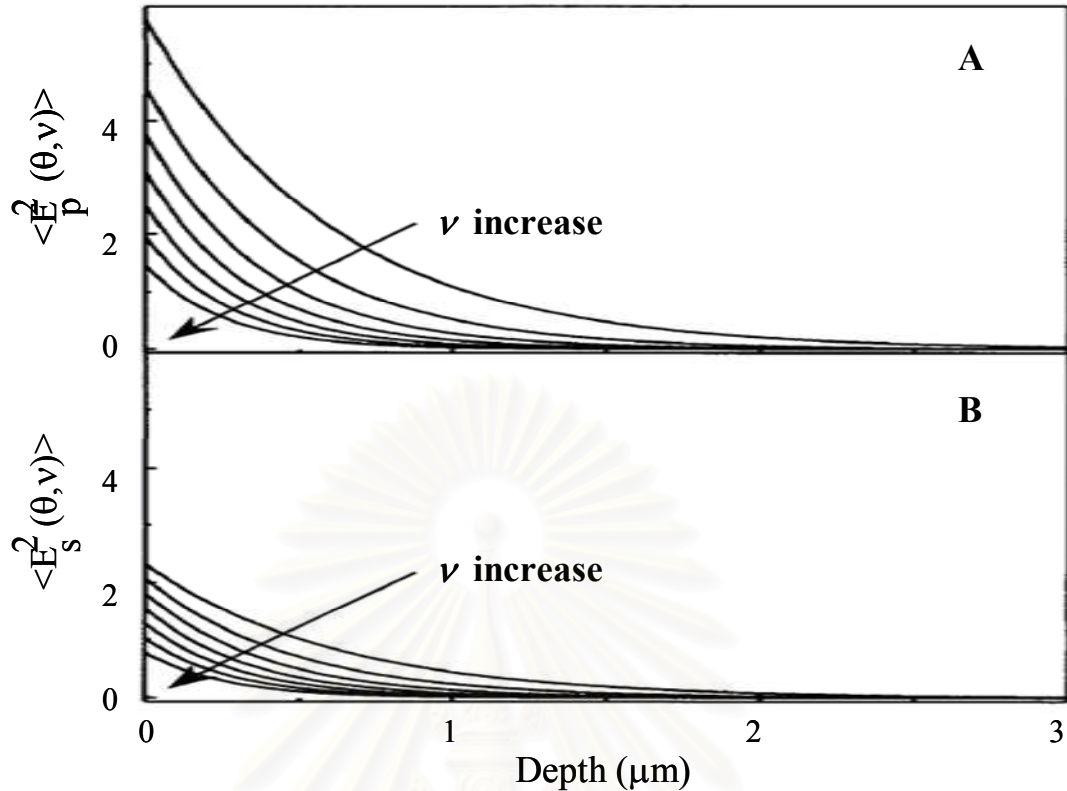


**Figure 2.6** Depth dependence MSEvF at various frequencies with (A) *p*-polarized radiation and (B) *s*-polarized radiation. The simulation parameters are  $n_0 = 4.0$ ,  $n_I = 1.5$ ,  $k_I = 0.0$ ,  $\theta = 45^\circ$ , and  $\nu = 500, 1000, 1500, \text{ and } 3000 \text{ cm}^{-1}$ .

The second thing to note about equation 2.8 is that the depth of penetration goes down as the refractive index of the IRE goes up. Thus, the Ge with a refractive index of 4.0 has a significantly shallower depth of penetration than that of a ZnSe IRE with a refractive index of 2.4. Changing IRE materials allows one to obtain spectra from different depths in a sample, which is known as depth profiling.

The denominator in equation 2.8 also includes the angle of incidence. Depth of penetration decreases as the angle of incidence of the infrared beam increases. The angle of incidence can be altered by varying the angle of the incoming radiation. However, the evanescent field depends strongly on the angle of incidence of the incident beam. The depth-dependent MSEvFs at various angles of incidence are shown in Figure 2.7. The MSEvF at the interface becomes smaller as the angle of incidence becomes larger. The angle of incidence also plays a major role in the decay



characteristic of the field. The greater the angle of incidence, the faster the decay of the field. As a result, the evanescent field at a greater angle of incidence decays to zero at a shallower depth than that of at a smaller angle. Some ATR accessories have movable mirrors that change the angle of incidence, so  $d_p$  can be varied controllably. Example of the penetration depth at various experimental conditions and material characteristics.

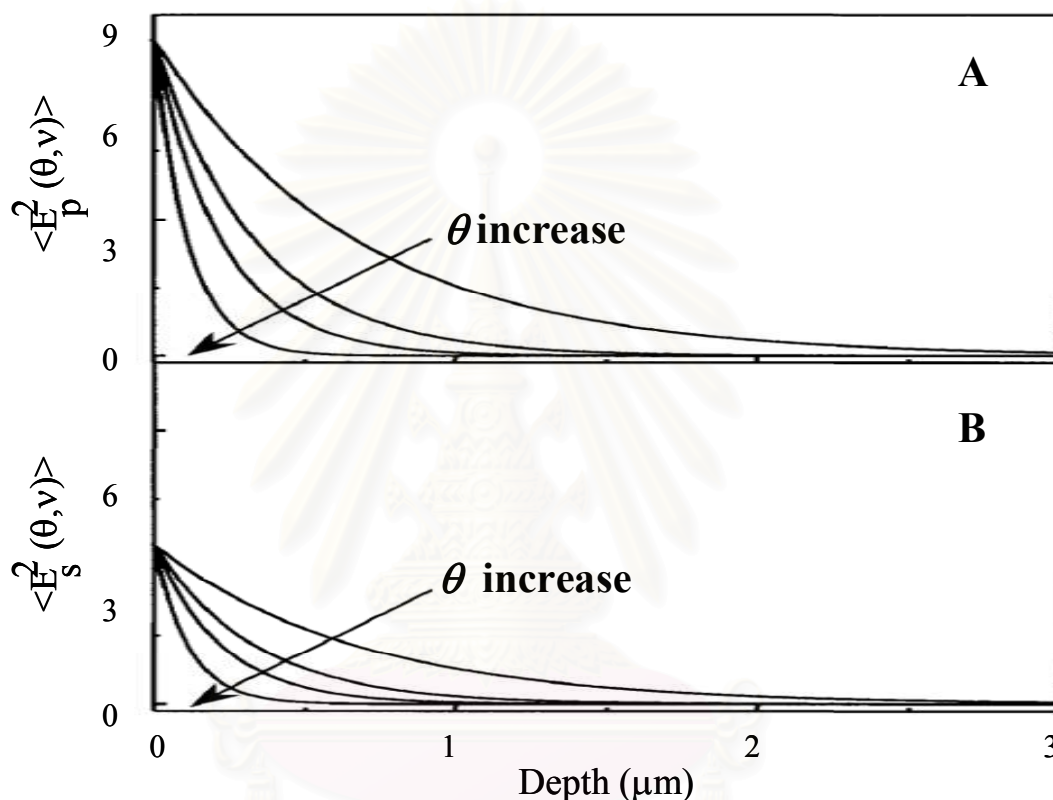


**Figure 2.7** Depth dependence MSEvF at various angles of incidence with (A)  $p$ -polarized radiation and (B)  $s$ -polarized radiation. The simulation parameter are  $n_0 = 4.0$ ,  $n_1 = 1.5$ ,  $k_1 = 0.0$ ,  $\nu = 1000 \text{ cm}^{-1}$ , and  $\theta = 30^\circ$ ,  $35^\circ$ ,  $40^\circ$ ,  $45^\circ$ ,  $50^\circ$ ,  $55^\circ$ , and  $60^\circ$ .

#### 2.2.4 Problem of Single Fiber in Conventional ATR Accessory

ATR FT-IR spectroscopy is a surface sensitive technique. However, it has several limiting applications. One of them is the contact area. The conventional hemispherical Ge IRE has a large sampling area ( $5 \times 5 \text{ mm}$ ). In order to obtain good ATR spectra, a very good alignment center of single human hair is required.

The small sample and single fiber rarely have an alignment center of sample especially the very small sample with comparing to the hemispherical IRE. When the sample does not align to the center of IRE, the smaller is the observed in spectral intensity. If the sample aligns to the out of sampling area of IRE, the spectrum cannot be observed.

Another limitation for ATR FT-IR spectroscopy is an optical contact between sample and IRE. When the system does not have an optical contact, there is always an air gap between the sample and the IRE. The larger the air gap, the smaller the observed in spectral intensity. If an air gap is large enough, the spectrum cannot be obtained. To solve this problem, the high pressure is applied at the sample against the IRE. However, the IRE maybe damaged by an excessive pressure.

## **2.3 ATR FT-IR Microspectroscopy**

### **2.3.1 Infrared Microscope**

Infrared microscopy involves the coupling of an FT-IR to a visible light microscope, and allows for visualizing and infrared examination of microscopic samples. Infrared microscopes are often incorporated high quality visible microscopes that have been re-designed for using with infrared radiation. A schematic diagram of a hypothetical infrared microscope is shown in Figure 2.8.

Infrared microscopes have become popular accessories during the past decade. These accessories are extremely versatile and can be used for a wide range of sample, only restrictions for microscope using are the size and hardness of the sample. The operation of microscope will be faster and easier than conventional technique due to fewer requirements for sample preparation. Their applications extend far beyond. It is important to use matching apertures for sample and background scans and always document the aperture size used. Also, most commercial microscope maybe used in transmission and reflection mode and with or without infrared polarizer. A broad range of newly applications have been developed around the imaging ability of the modern microscopes in combination with computer video graphics and computer controlled sampling stages [46].

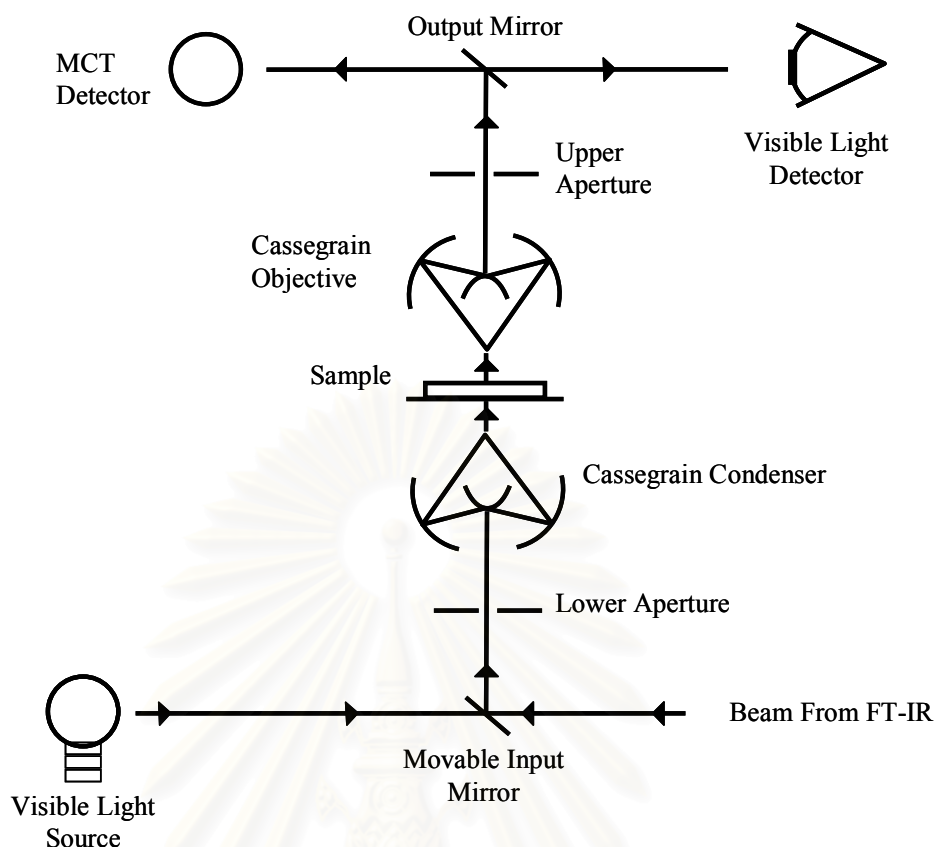


**Figure 2.8** An optical diagram of an infrared microscope.

### 2.3.2 Homemade Slide-on Ge IRE Accessory

The homemade slide-on Ge  $\mu$ IRE was developed by Sensor Research Unit, Department of Chemistry, Faculty of Science, Chulalongkorn University, for the analysis of the small amount sample or single fiber. Due to the small sample area of the IRE, spectra of single hair showed the superb spectral quality and wide applications in analysis of other sample.

### 2.3.2.1 Ray Tracing of Homemade Slide-on Ge IRE

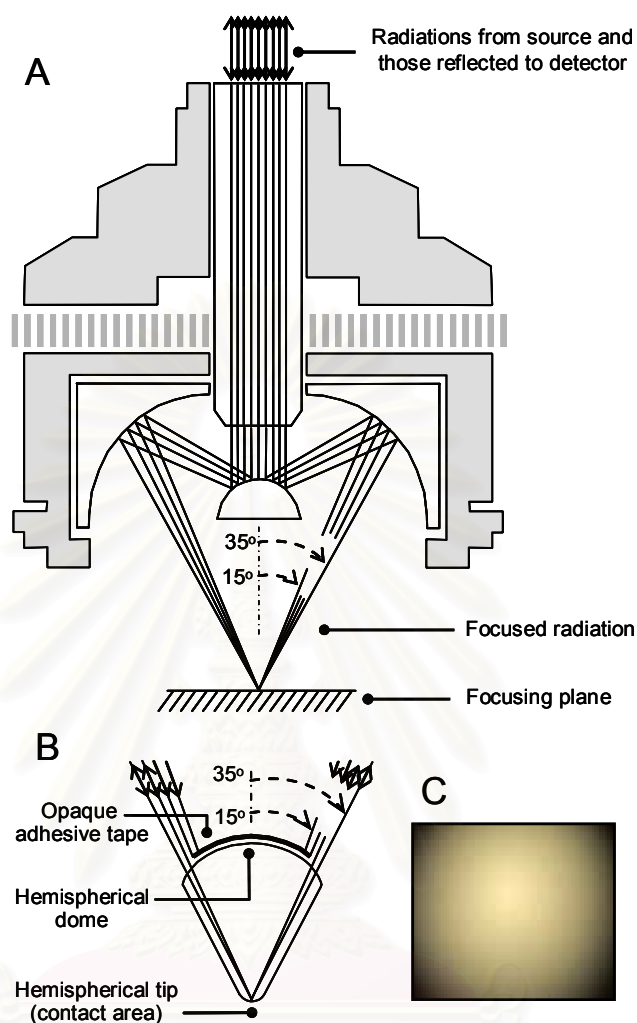


**Figure 2.9** A schematic illustration of ray tracing within the 15 X Schwarzschild Cassegrain infrared objective.

A schematic illustration of ray tracing within the 15X Schwarzschild Cassegrain infrared objective and the coupling of the focused radiation into the homemade slide-on Ge  $\mu$ IRE are shown in Figure 2.9. The concave primary mirror and the convex secondary mirror of the objective focus radiation onto the reflecting plane with angles of incidence ranging from  $15.6^\circ$  to  $35.5^\circ$ , Figure 2.9A. By coupling the focused radiation into a specially designed  $\mu$ IRE made of high refractive index materials and by making the angle of incidence at the sampling surface greater than the critical angle, a spectral acquisition under the ATR FT-IR condition can be obtained.

The hemispherical dome of the miniature cone-shaped Ge  $\mu$ IRE facilitates the coupling of the focused radiation traveling into the  $\mu$ IRE by minimizing the reflection loss at the air/Ge interface, Figure 2.9B. If a nearly perfect coupling was assumed, the radiation transmitted through the air/Ge interface of the dome and impinged the Ge/air interface of the tip without a significant change in the angle of incidence (i.e., the refraction at the air/Ge interface was minimized). To ensure a good contact between the Ge tip and a solid sample, the circular tip of the IRE was made a hemispherical surface. Since the contact area is small ( $\sim 100 \mu\text{m}$  in diameter, Figure 2.9C), a good contact was achieved with a minimal force exerting on the tip.



สถาบันวิทยบริการ  
จุฬาลงกรณ์มหาวิทยาลัย

## CHAPTER III

### EXPERIMENTAL SECTION

The study of human hair by the homemade slide-on Ge  $\mu$ IRE accessory was performed. The accessory was employed for analysis of single human hair and trace cosmetics on the surface of single human hair. This technique is easy for the analysis of single human hair because of the small sampling area of the IRE without sample preparation. The application of the homemade slide-on Ge  $\mu$ IRE accessory was demonstrated for forensic analysis of human hair.

#### 3.1 Materials and Equipments

##### 3.1.1 Samples

- Untreated-hairs from the volunteers with different factors such as age, sex, diameter of hair, and color
- Chemical treated-hairs
  - Straight creams treated-hair
  - Permanent wave lotion treated-hair
  - Color creams treated-hair
- Split hairs

##### 3.1.2 Instruments

1. Nicolet Magna 750 FT-IR spectrometer equipped with a mercury-cadmium-telluride (MCT) detector.
2. NICPLAN<sup>TM</sup> infrared microscope with 15X Cassegrain infrared objective and 10X glass objective.

3. Single-reflection attenuated total reflection accessory (The Seagull™, Harrick Scientific, USA) with a hemispherical Ge IRE.
4. Homemade slide-on germanium (Ge)  $\mu$ IRE

### 3.2 Default Spectral Acquisition

#### Nicolet Magna 750 FT-IR Spectrometer

##### Instrumental Setup

Source	Standard Globar™ Infrared Light Source
Detector	MCT/A
Beam splitter	Ge-coated KBr

##### Acquisition Parameters

Spectral resolution	4 $\text{cm}^{-1}$
Number of scans	512 scans
Spectral format	Absorbance

##### Advanced Parameters

Zero filing	none
Apodization	Happ-Genzel
Phase correction	Mertz

#### NICPLAN™ Infrared Microscope

##### Instrumental Setup

Objective	15X Schwarzschild-Cassegrain
Aperture size	100 x 100 $\mu\text{m}^2$

### 3.3 Homemade Slide-on Ge $\mu$ IRE Accessory

The homemade slide-on Ge  $\mu$ IRE accessory consists of two components including the Ge slide-on IRE and the slide-on housing (Figure 3.1).



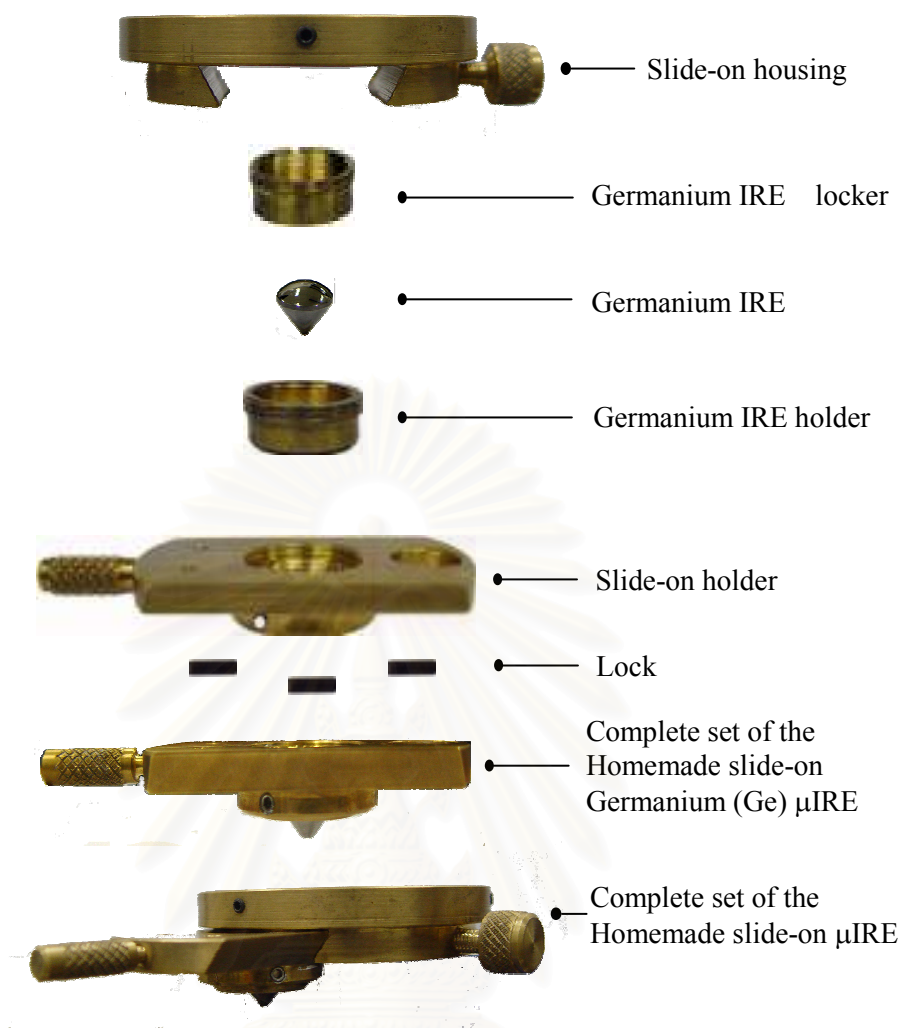


**Figure 3.1** The homemade slide-on Ge  $\mu$ IRE accessory was developed by Sensor Research Unit, Department of Chemistry, Faculty of Science, Chulalongkorn University, Bangkok 10330, Thailand.

The homemade slide-on Ge  $\mu$ IRE consists of the dome-shaped Ge  $\mu$ IRE which designed for characterizing the small sample. The Ge  $\mu$ IRE was fixed into the slide-on holder by Ge IRE locker as shown in Figure 3.1. A homemade slide-on Ge  $\mu$ IRE was aligned to achieve ATR spectrum and high energy throughput by Ge IRE holder and three knobs. Another component is the slide-on housing which fixed on NICPLAN<sup>TM</sup> infrared microscope.

The homemade slide-on Ge  $\mu$ IRE accessory was slid into the position on the slide-on housing at NICPLAN<sup>TM</sup> infrared microscope as shown in Figure 3.2. The

incident infrared radiation from the microscope was coupled onto the hemispherical dome of the Ge  $\mu$ IRE and focused at the tip of Ge  $\mu$ IRE.



**Figure 3.2** The homemade slide-on Ge  $\mu$ IRE accessory mounted onto the infrared microscope.

### 3.4 Characterization of Single Human Hair by ATR FT-IR Spectroscopy

#### 3.4.1 Experimental Procedure for the Conventional ATR Accessory

A commercial single reflection ATR accessory (the Seagull<sup>TM</sup>, Harrick Scientific, USA) with a hemispherical Ge IRE (diameter 25 mm) was employed for ATR spectral acquisition of a single hair. A hemispherical Ge IRE was mounted into the ATR accessory. The angle of incidence was 30°. The spectrum obtained by the Ge IRE without sample was employed as a background for all acquired ATR FT-IR spectra. To collect a spectrum of single hair, the hair sample was rinsed with acetone and dried under room temperature overnight and placed on a metal substrate with the hair thread aligned along the center of the IRE. The substrate was then raised until the hair touched the flat surface of the IRE with an applied pressure, as shown in Figure 3.3. The same procedure was repeated for all other hair samples.

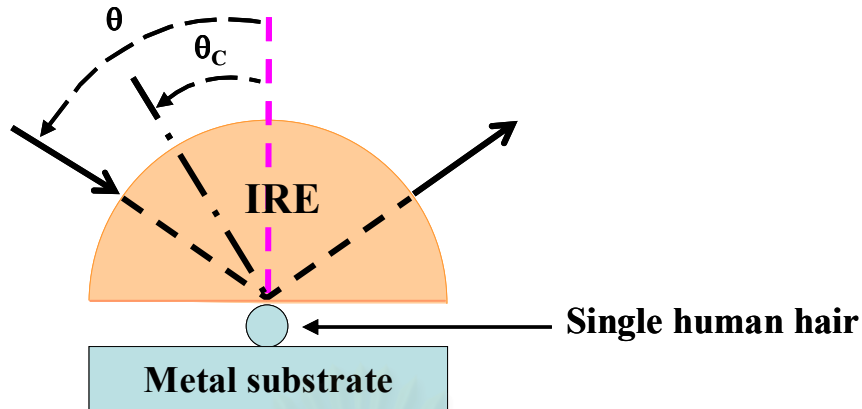


**Figure 3.3** Experimental procedures for ensuring the optical contact between a sample and the IRE of the conventional ATR accessory.

#### **3.4.2 Experimental Procedure for the Homemade Slide-on Ge $\mu$ IRE Accessory.**

All ATR spectra were performed via a NICPLAN<sup>TM</sup> infrared microscope equipped with a mercury-cadmium-tellurium (MCT) detector that attached to the Nicolet Magna 750 FT-IR Spectrometer. A homemade slide-on Ge  $\mu$ IRE accessory was employed for all spectral acquisitions. The homemade slide-on Ge  $\mu$ IRE accessory was aligned and fixed at the optimum position of slide-on housing where the contact tip coincided with the focal point of the built-in 15X Cassegrain infrared objective. The spectral acquisitions were performed in the reflection mode of infrared microscope. For spectral acquisition of a hair sample, the hair sample was fixed to a mounting plate at both ends and the plate was held on the microscope stage, after the hair was rinsed with acetone. A sampling spot on the hair was selected through a built-in objective (optical or infrared). The homemade slide-on Ge  $\mu$ IRE accessory was slid into the optimum position of slide-on housing and the microscope stage was elevated until the selected position touched the tip of the IRE as shown in Figure 3.4. The same procedure was repeated for all other hair samples.

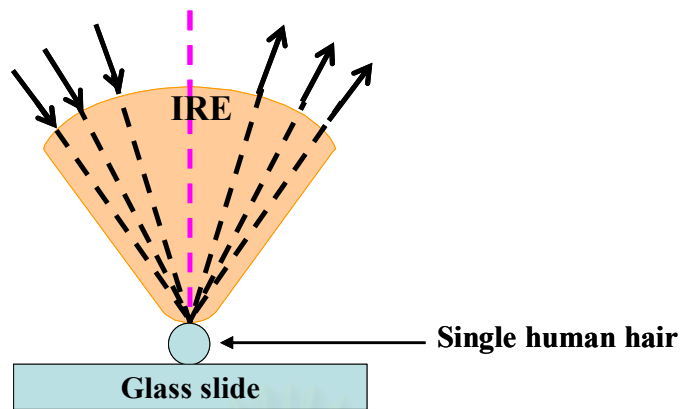


**Figure 3.4** Experimental procedures for ensuring the optical contact between a sample and the IRE of the homemade slide-on Ge  $\mu$ IRE accessory.

In this section, the different positions of the hair were collected with two experiments. Firstly, ATR FT-IR spectra at various interesting positions along the hair filament with an interval of 1.5 cm were collected. The first spectrum was taken at 1.5 cm from the scalp hair, as shown in Figure 3.5. Secondly, ATR FT-IR spectra of hair at various positions on the head were collected. Area on one head was divided into four parts and the three hair filaments were randomly analyzed for each part as seen in Figure 3.6.

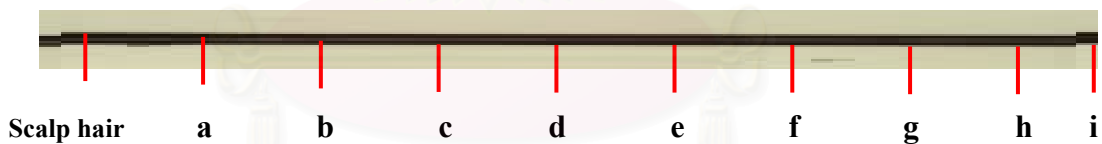


**Figure 3.5** The sampling positions along the single human hair in the first experiment.

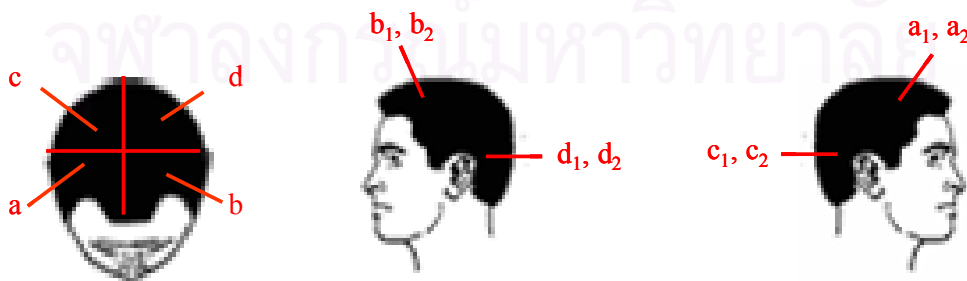


**Figure 3.6** Single human hair from various positions on a head were analyzed in the second experiment.

### 3.5 Characterization of Trace Cosmetic on the Hair Surface

The novel technique called “*Contact-and-Collect*” was developed for the measurement of trace cosmetics on the surface of single human hair (i.e., shampoos, hair conditioners and hair treatment cosmetics).

#### 3.5.1 Experimental Procedure for the Conventional ATR Accessory

A commercial single reflection ATR accessory (the Seagull™, Harrick Scientific, USA) with a hemispherical Ge IRE (diameter 25 mm) was employed for ATR spectral acquisition of a single hair. A hemispherical Ge IRE was mounted into the ATR accessory and the angle of incidence was set at 30°. The hair sample was placed on a metal substrate with the hair thread aligned along the center of the IRE. The hair sample on a metal substrate was then raised until the hair touched the flat surface of the IRE with applied pressure as shown in Figure 3.7A. When the hair sample was contacted the IRE, the cosmetic on surface of hair can be characterized with combining the interference of hair, as shown in Figure 3.7B. After removing the hair, some of the cosmetics on the hair surface stuck onto the IRE surface. The trace amount of the cosmetics on the IRE can be characterized under the ATR mode without any interference of hair, as shown in Figure 3.7C.

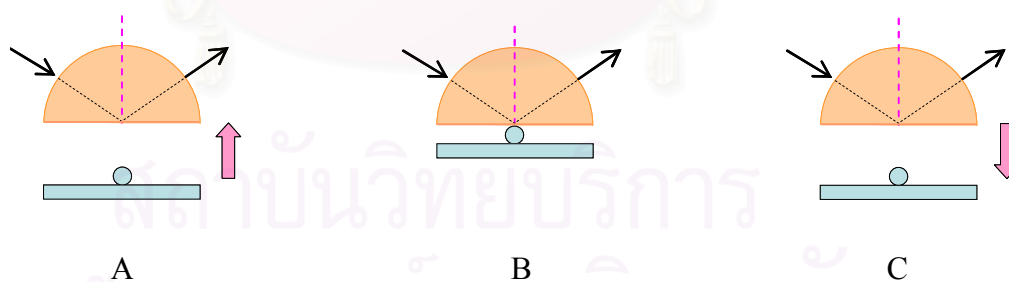


**Figure 3.7** Experimental procedures for spectral acquisition using *Contact-and-Collect* technique by the hemispherical Ge IRE: (A) the hair sample was raised until the hair touched the IRE with applied pressure, (B) the hair sample was contacted the IRE and characterized the cosmetics and hair, and (C) the hair sample was removed from the IRE and characterized the cosmetic without interference of hair.

### 3.5.2 Experimental Procedure for the Homemade Slide-on Ge $\mu$ IRE Accessory.

All ATR spectra were performed on a NICPLAN<sup>TM</sup> infrared microscope equipped with a mercury-cadmium-tellurium (MCT) detector that attached to the Nicolet Magna 750 FT-IR Spectrometer. A homemade slide-on Ge  $\mu$ IRE accessory was employed for all spectral acquisitions. The IRE was aligned and fixed at the optimum position of the slide-on housing where the contact tip coincided with the focal point of the built-in 15X Cassegrain infrared objective. The spectral acquisitions were performed in the reflection mode of infrared microscope. For spectral acquisition of samples, hair sample was placed on a glass slide and positioned on the microscope stage, after the hair was rinsed with acetone. A sampling spot on the hair was selected through a built-in objective (optical or infrared objective). The homemade slide-on Ge  $\mu$ IRE accessory was slid into the optimum position of the slide-on housing and the microscope stage was elevated until the selected position touched the tip of the  $\mu$ IRE, as shown in Figure 3.8A. When the hair sample was contacted with the IRE, the cosmetic on surface of hair can be characterized with combining the interference of hair, as shown in Figure 3.8B. After removing the hair, some of the cosmetics on the hair surface stuck onto the  $\mu$ IRE. The trace amount of the cosmetics on the IRE can be characterized under the ATR mode without any interference of hair, as shown in Figure 3.8C. Several contacts can be performed in order to collect a sufficient amount of the trace cosmetics on the tip of the  $\mu$ IRE for getting a good quality spectrum.



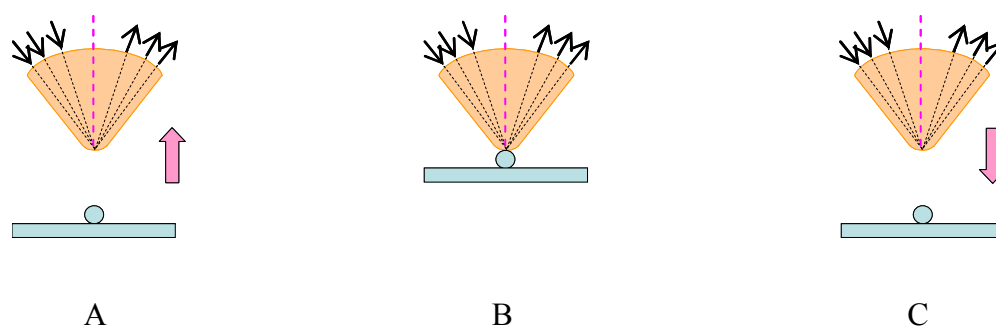


**Figure 3.8** Experimental procedure for spectral acquisition using *Contact-and-Collect* technique by the homemade slide-on Ge  $\mu$ IRE accessory: (A) the hair sample was raised until the hair touched the IRE with applied pressure, (B) the hair sample was contacted the IRE and characterized the cosmetics and hair, and (C) the hair sample was removed from the IRE and characterized the cosmetic without interference of hair.

### 3.6 Characterization of Split Hairs by ATR FT-IR Microspectroscopy

#### 3.6.1 Experimental Procedure for the Homemade Slide-on Ge $\mu$ IRE Accessory.

All ATR spectra were performed on a NICPLAN<sup>TM</sup> infrared microscope equipped with a mercury-cadmium-tellurium (MCT) detector that attached to the Nicolet Magna 750 FT-IR Spectrometer. A homemade slide-on Ge  $\mu$ IRE accessory was employed for all spectral acquisitions. The IRE was aligned and fixed at the optimum position of the slide-on housing where the contact tip coincided with the focal point of the built-in 15X Cassegrain infrared objective. The spectral acquisitions were performed in the reflection mode of infrared microscope. For spectral acquisition of samples, hair sample was deposited on glass slide and placed on the microscope stage. The homemade slide-on Ge  $\mu$ IRE accessory was slid into the optimum position of the slide-on housing and the microscope stage was elevated until the selected position touched the tip of the IRE.

Figure 3.9 shows the various positions of split hairs collected in this section. The initial position of splitted hair at 0 position was set as reference point. From the reference position, the various positions before splitted position of hair was taken at

1.0 cm along the hair as shown at  $b_1$ ,  $b_2$ ,  $b_3$ , respectively. After splitting position, the hair was divided into two filaments. One hair filament has a large in diameter and the other hair filament has a small in diameter. The sampling positions of large hair filament are labeled as follows:  $a_1$ ,  $a_2$ ,  $a_3$ , respectively while those of small hair filament are  $a'_1$ ,  $a'_2$ ,  $a'_3$ , respectively.

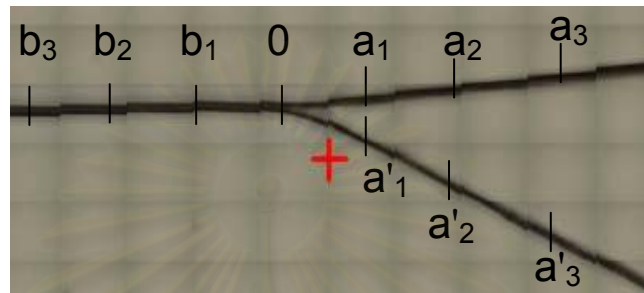


**Figure 3.9** The sampling positions split hairs by the homemade slide-on Ge  $\mu$ IRE accessory.

## CHAPTER IV

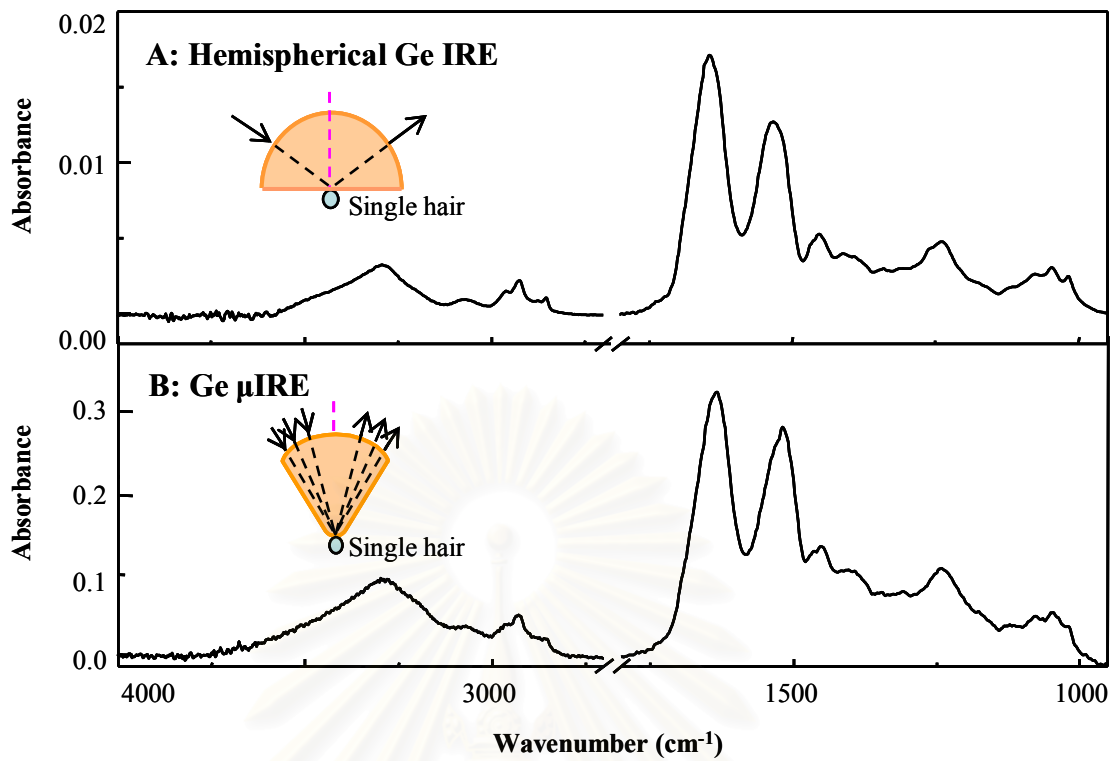
### RESULTS AND DISCUSSION

The chemical information of single human hair, the difference of spectrum between untreated and treated single human hair, the spectra of cosmetic on the surface of single human hair, and the variation of the spectra of un-split hair and split hair were determined.

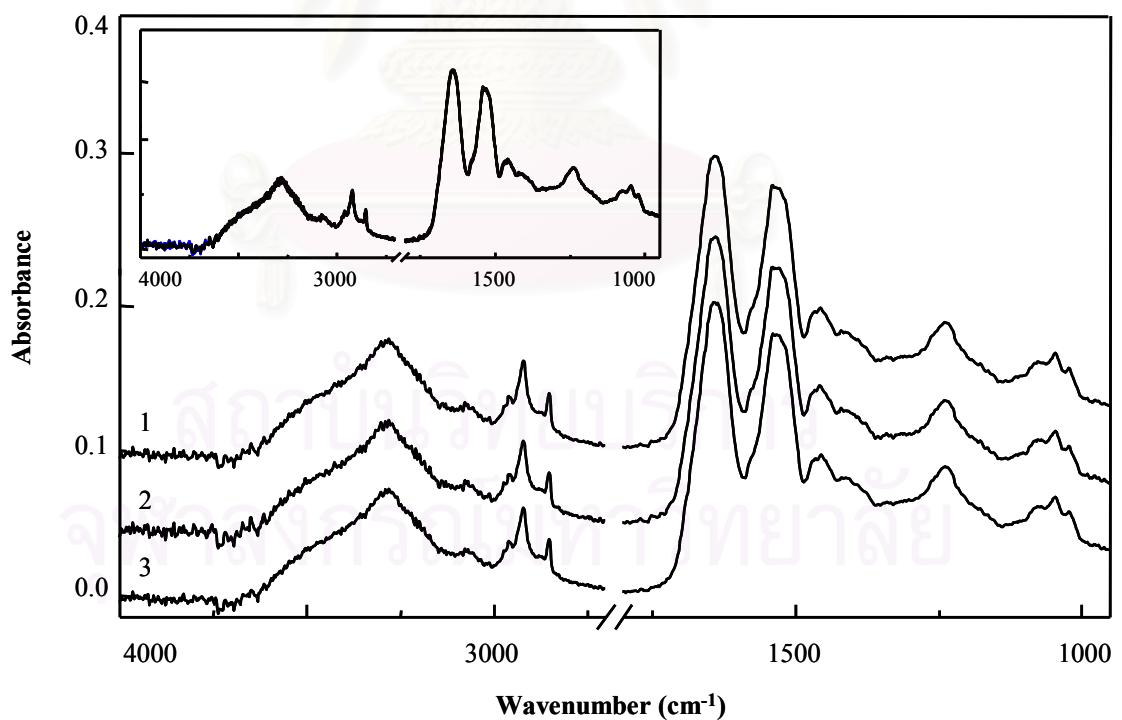
#### 4.1 Efficiency of Homemade Slide-on Ge $\mu$ IRE Accessory

Figure 4.1 shows the spectral of a single human hair acquired by the hemispherical conventional ATR and the homemade slide-on Ge  $\mu$ ATR. Although these spectra reveal the same spectral features, the spectrum acquired by the homemade slide-on Ge  $\mu$ IRE accessory has a better signal-to-noise ratio (SNR) and shows higher spectral intensity. Since the homemade slide-on Ge  $\mu$ IRE accessory has small sample area, the good contact between the sample and IRE was achieved. The position on the hair can be selected via objective of microscope. All the analysis of hair is easy without an additional sample preparation, non-destructive and short analysis time.

In order to ensure the reproducibility of the homemade slide-on Ge  $\mu$ IRE, the observed spectra of single human hair from the individual person and same position were compared. The typical results are shown in Figure 4.2. The insert shows the superimposition when the spectra was normalized by Amide I band at  $1637\text{ cm}^{-1}$ .



**Figure 4.1** ATR FT-IR spectra of single human hair acquired by: (A) Conventional Ge IRE and (B) Homemade slide-on Ge  $\mu$ IRE accessories.



**Figure 4.2** Normalized ATR FT-IR spectra of single hair from a person at three positions. The insert were normalized spectra by Amide I absorption band ( $1637\text{ cm}^{-1}$ ).

## 4.2 Chemical Information of Human Hair

The main components of human hair included the primary protein, water, lipid, wax. The ATR FT-IR spectrum of single human hair acquired by homemade slide-on Ge  $\mu$ IRE accessory was shown in Figure 4.3. The observed spectrum shows a broad band at  $3274\text{ cm}^{-1}$  attributed to O-H stretching of water together with N-H stretching vibration. The predominant absorption bands at  $1637$ ,  $1521$  and  $1226\text{ cm}^{-1}$  related to Amide I, Amide II and Amide III vibrations, respectively. The C=O stretching vibration and a small contribution from N-H scissoring vibration correspond to Amide I vibration. The absorption bands of Amide II vibrational mode consist of two components including the C-N stretching and N-H wagging vibration while the N-H twisting vibration mode plus C-N stretching and the contribution from O=C-N bending vibration is that of Amide III.

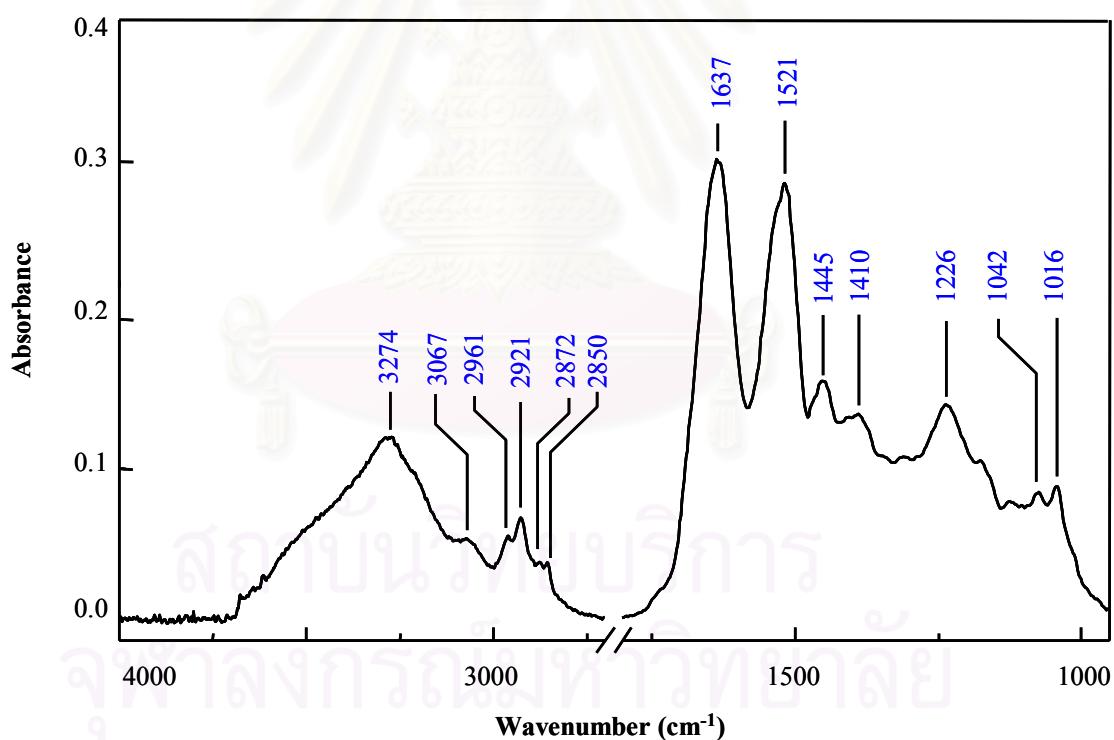


**Figure 4.3** ATR FT-IR spectrum of single hair.

The absorption bands at  $2961$ - $2850\text{ cm}^{-1}$ ,  $1445$  and  $1410\text{ cm}^{-1}$  are the C-H stretching and C-H deformation vibration, respectively. The IR peak assignments were summarized in Table 4.1.

**Table 4.1 Peak assignments of human hair [32, 52, 53]**

Wavenumber (cm <sup>-1</sup> )		Assignments
Literature [32]	Current work	
3370-3320	3274	Asymmetric N-H stretching
2975-2950	2961	Asymmetric C-H stretching of CH <sub>3</sub>
2940-2915	2921	Asymmetric C-H stretching of CH <sub>2</sub>
2885-2865	2872	Symmetric C-H stretching of CH <sub>3</sub>
2870-2840	2850	Symmetric C-H stretching of CH <sub>2</sub>
1680-1630	1637	Amide I C=O stretching and a small contribution from N-H bending (scissoring)
1550-1510	1521	Amide II C-N stretching plus N-H bending (wagging)
1305-1200	1226	Amide III N-H bending (twisting) plus C-N stretching and contribution from O=C-N bending
1480-1440	1445	C-H bending (scissoring) of CH <sub>2</sub>
1410-1350	1410	C-H bending (wagging) of CH <sub>3</sub>
1070-1035	1042	S=O stretching of cysteic acid

### 4.3 Characterization of Single Human Hair by ATR FT-IR Microspectroscopy

The characterization of single human hair is the significant aspect of the biological analysis, forensic analysis, and cosmetic industrial analysis. Human hairs have a specific character of protein structure in individual person. Each person has a different genetic, life style, cosmetic used, dietary, and healthy [47]. Results of hair spectra mentioning in prior section—homemade slide-on Ge  $\mu$ IRE accessory can be characterized the chemical information of single human hair. Thus, this technique is suitable for hair analysis.



### 4.3.1 Untreated-Hair

In the present study, single human hair was collected from persons with different age, gender, and color. This study was divided into sections to study the parameters affecting hair quality.

#### 4.3.1.1 ATR FT-IR Spectra of Hairs from Different Persons with Different Ages

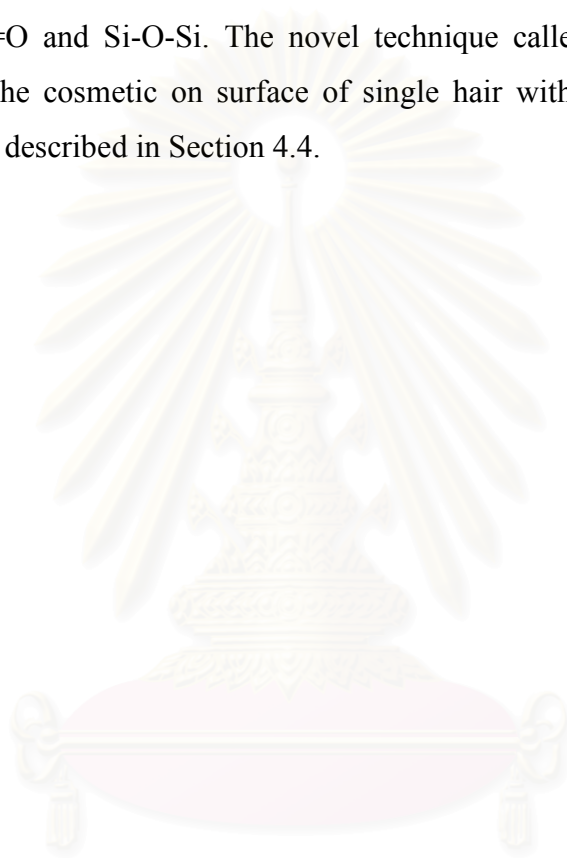
Figure 4.4 shows the different spectra of single human hair acquired from person with different age. Each observed spectrum shows the different peak positions and peak shape at 1637, 1521, and 1226  $\text{cm}^{-1}$  assigned to absorption vibration of Amide I, II and III. As clearly seen in the insert of Figure 4.4, ATR FT-IR spectra show significant variation of protein component in each person. Due to the qualities of the hair are associated with the hair composition, hair's treatment (i.e., ultraviolet (UV) irradiation, brushing, drying, and heating), dietary, and healthy of the person, these factors are believed to cause hair damage. The protein bond in human hair was changed by these factors.

Obtaining the different spectra, it means that the chemical structure of hair is changed by these factors. The observed spectrum of hair can be used in uniquely characterization and applied in forensic analysis. However, the chemical structure of hair does not depend on age, thus age of hair has no influence on chemical structure of hair [32].

#### 4.3.1.2 ATR FT-IR Spectra of Hairs from Male and Female

The observed spectra in Figure 4.5 show the variation of spectral features from persons due to the effect of gender. The observed spectra show the dominant different peak positions at 1637, 1521, and 1226  $\text{cm}^{-1}$  associated with absorption vibration of Amide I, II and III. The spectrum of hair from male and female can be characterized by the different spectrum of each person. Since the genetic was influenced on the cystine content of human hair (i.e. higher levels of this amino acid has been reported in hair from male individual than that of female) [32].

The hair from the same gender shows different spectrum because the specific character of protein in each person that affecting from component of protein in the hair, hair treatment dietary, and healthy of the person. A slight difference of absorption band at 1042 and 1017  $\text{cm}^{-1}$  related with the absorption of S=O (domain structural protein in human hair) and Si-O-Si of silicone oil being main component of cosmetic hair treatment, respectively. These two bands are interfering. From this study, it is concluded that the ATR FT-IR spectra were used for differentiation between the S=O and Si-O-Si. The novel technique called “*Contact-and-Collect*” could analyze the cosmetic on surface of single hair without an additional sample preparation that described in Section 4.4.



สถาบันวิทยบริการ  
จุฬาลงกรณ์มหาวิทยาลัย

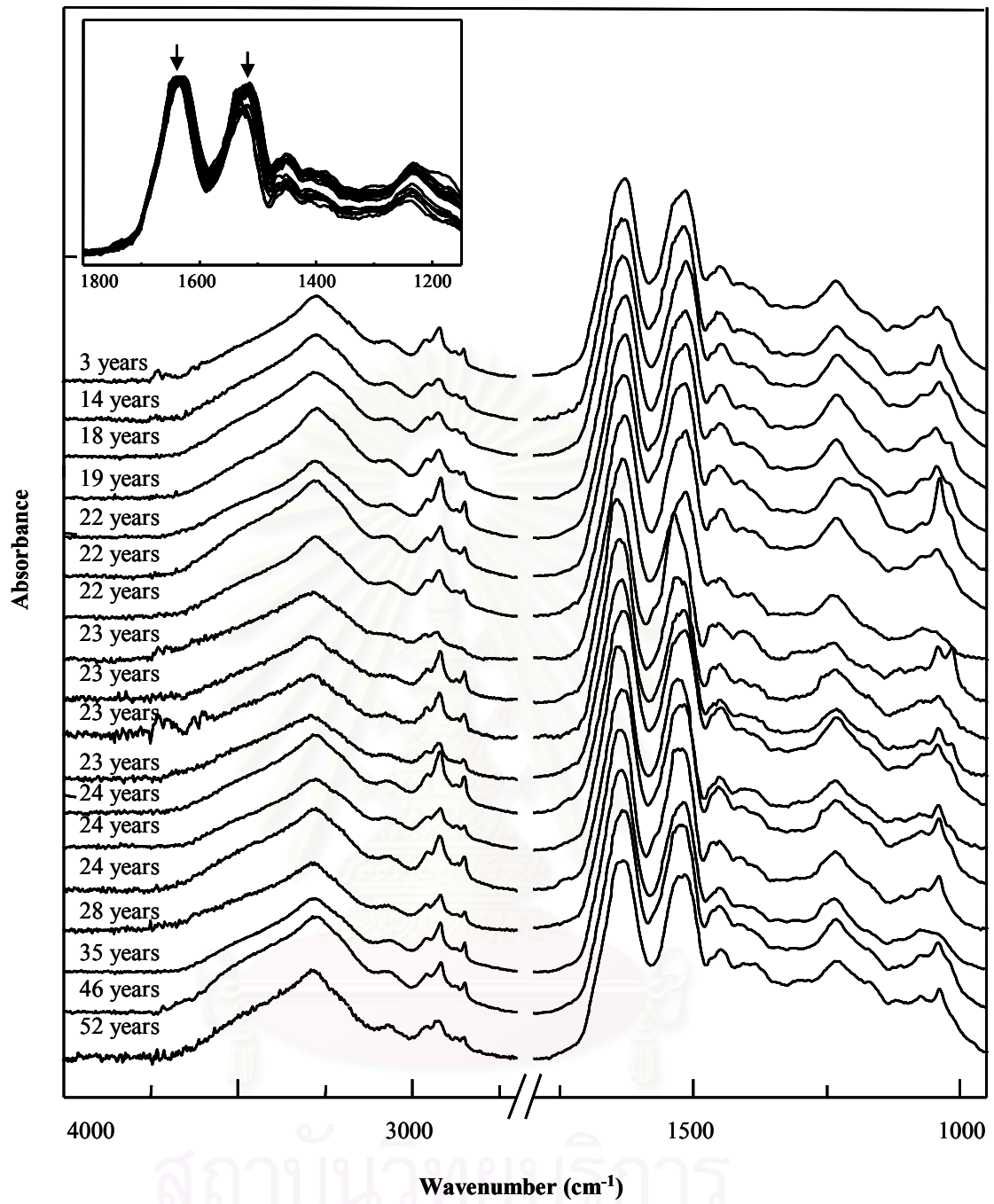


**Figure 4.4** ATR FT-IR spectra of human hair from different persons.

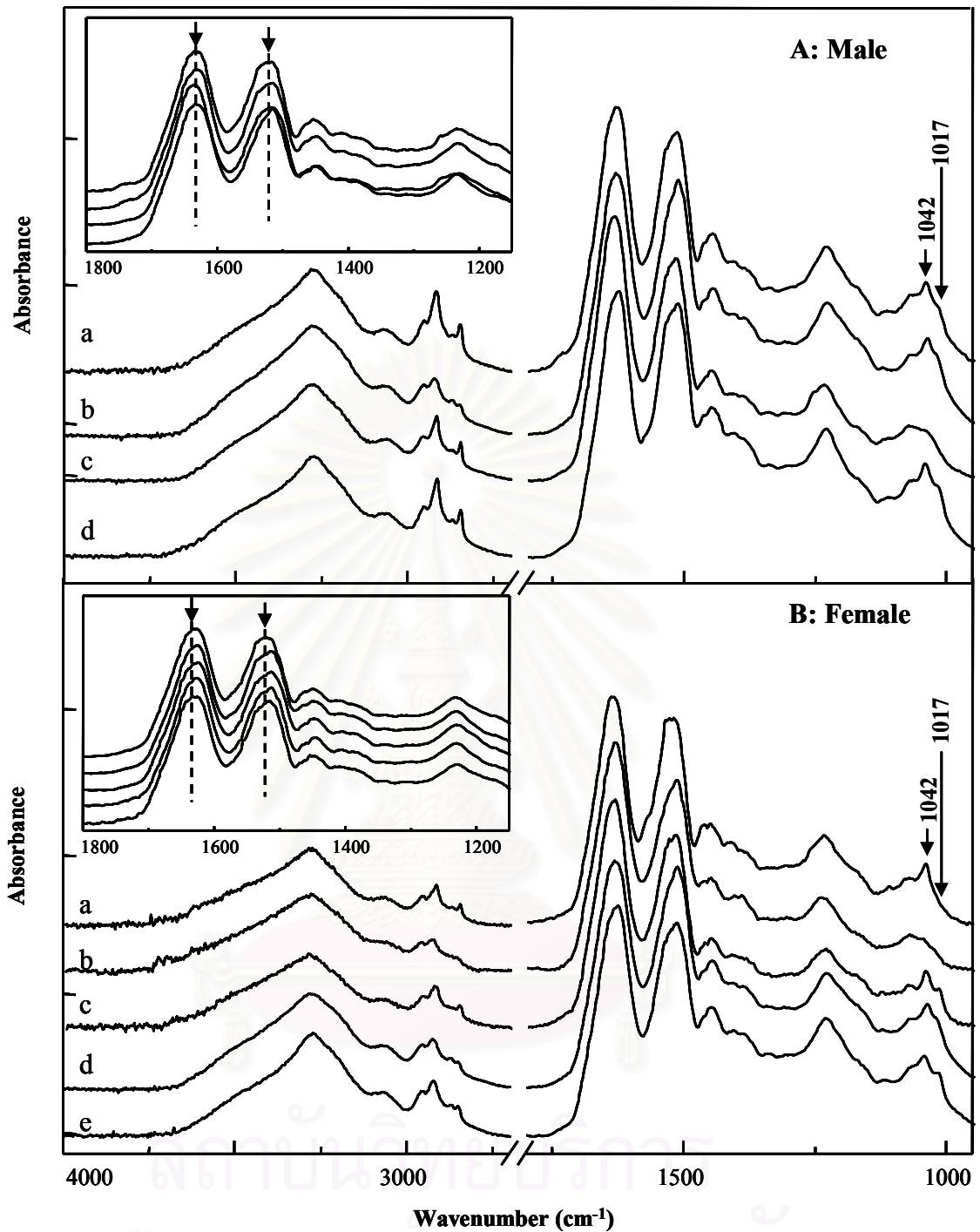


**Figure 4.5** ATR FT-IR spectra of single human hair from persons with different gender: (A) males and (B) females.

#### 4.3.1.3 ATR FT-IR Spectra of Hairs from the Individual Person with Different Natural Hair Color

The occurrence of the color of hair comes from the presence of pigment in cortex layer of human hair. The pigment cells called “melanin” create a black

pigment. The greater amount of pigment in the hair, the hair color becomes dark. On the other hand, the amount of pigment is reduced, the hair color turns brown and then blonded.

Figure 4.6 shows the ATR FT-IR spectra of single human hair from the individual person with different natural hair color acquired by the homemade slide-on Ge  $\mu$ IRE. The observed spectrum shows the same spectral feature. The hair from individual person was not affected from the hair composition, hair treatment (i.e., ultraviolet (UV) irradiation, brushing, drying, and heating), dietary, and healthy of the person. The difference quality of melanin in different color cannot be detected by infrared spectrum in mid-IR region but those were shown in near-IR [33]. Thus, the color of hair was natural changed having no influence on spectrum of hair acquired by ATR FT-IR technique. The spectra in 1040-1020  $\text{cm}^{-1}$  region reveal the difference of spectral features due to the quality of cosmetic from hair treatment such as shampoo, conditioner, spray, mousses, and others. These absorption band of the cosmetic are interfering with S=O vibration which found in the protein structure in human hair. However, the different bands at 1040 and 1020  $\text{cm}^{-1}$  can be differentiated by the “*Contact-and-Collect*” technique.

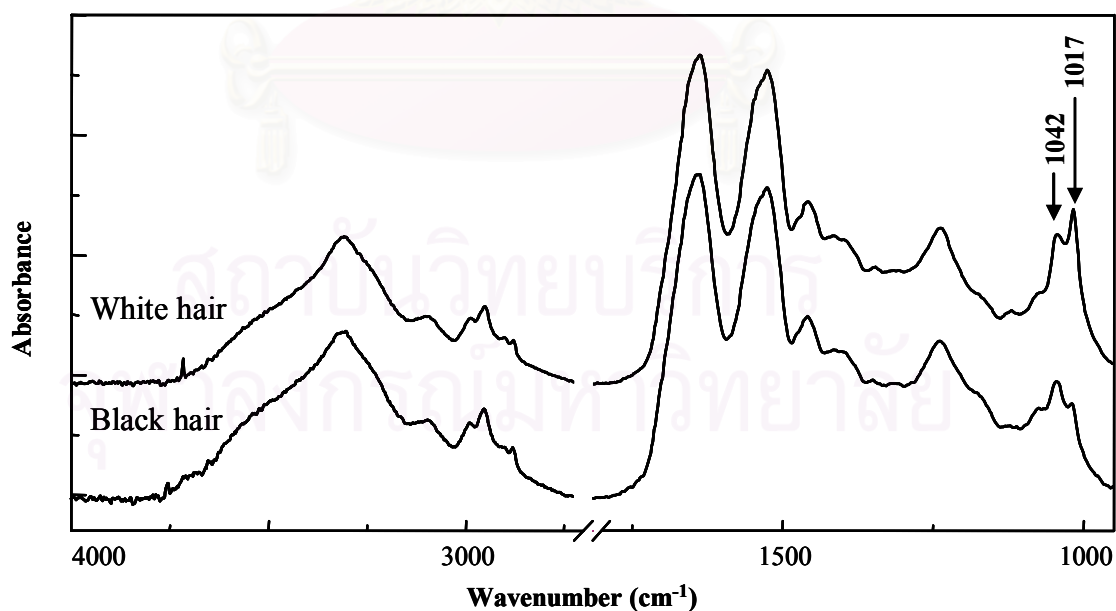
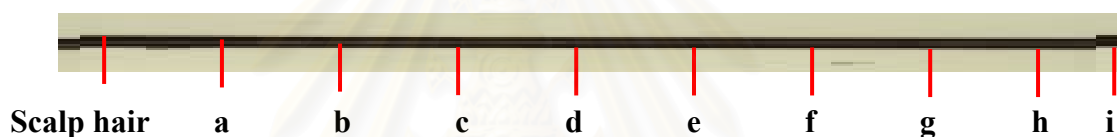


**Figure 4.6** ATR FT-IR spectra of hair from individual person with different natural hair color.

As the results, ATR FT-IR spectra of single human hair show the specific character of structural protein in each person due to the ratio of protein component from genetic, chemical treatment (i.e., ultraviolet (UV) irradiation, brushing, drying, and heating), diet, and health of the person. These different spectra of single hair can be employed for unique identification or differentiation of hair based on the observed spectra that associated with the molecular structure of hairs. Therefore, the “*Contact-and-Collect*” technique can be applied for forensic analysis.

#### 4.3.1.4 ATR FT-IR Spectra of Hairs from Different Position along the Hair Filament and Different Position of hair on Head

##### The different position along the hair filament



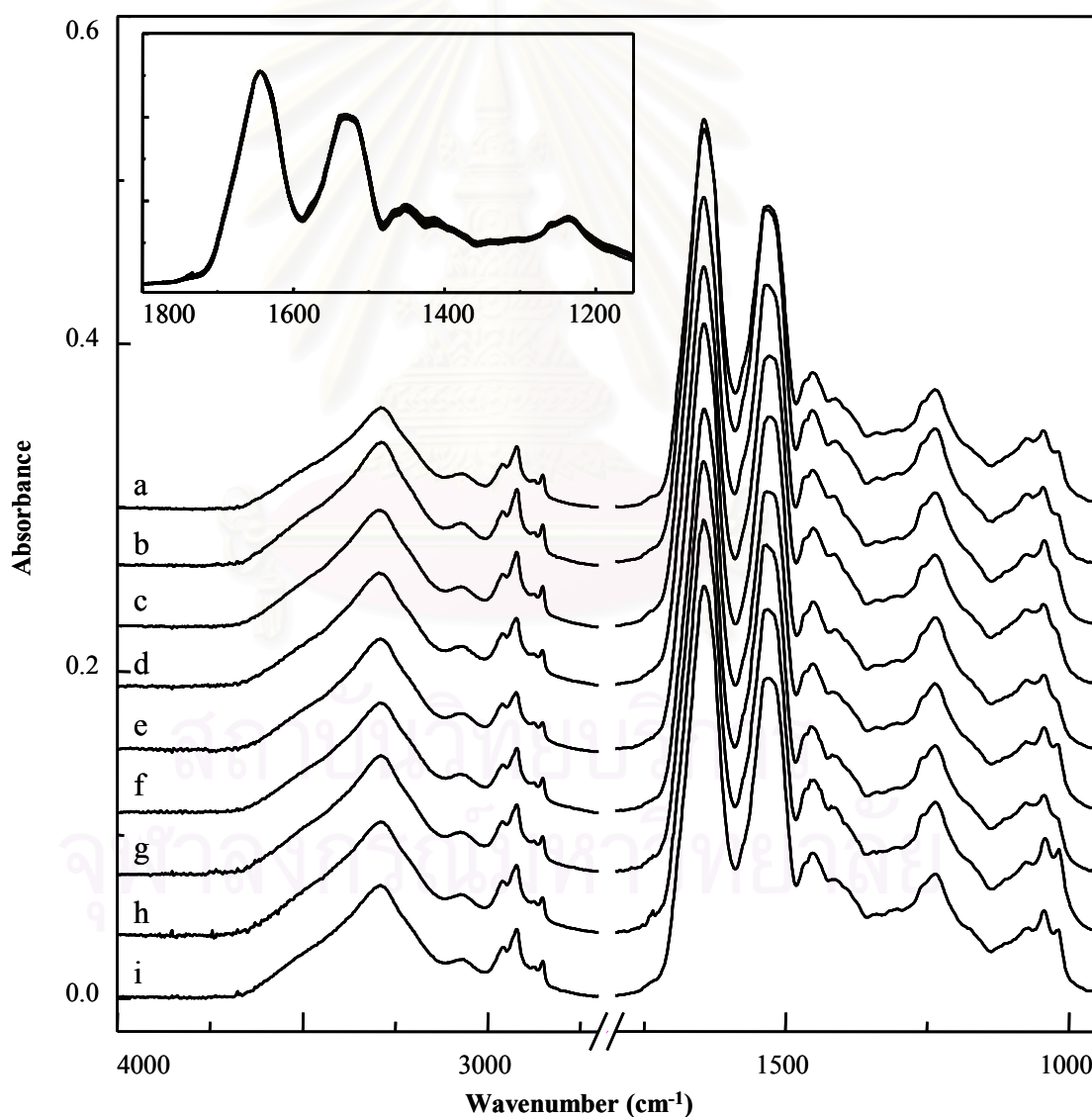
**Figure 4.7** The sampling positions along the single human hair.

Figure 4.8 shows ATR FT-IR spectra acquired from a single human hair. The spectra were collected along the hair filament with an interval of 1.5 cm. The first spectrum was taken at 1.5 cm from the scalp hair. Each position along the hair filament of individual person shows the same spectral feature. The insert shows the superimposition when the spectra were normalized by Amide I band at  $1637\text{ cm}^{-1}$ . Due to the specific character of hair and effect from the hair damage such as environment (i.e., ultraviolet (UV) irradiation, brushing, drying, and heating), dietary, and healthy of the person cannot be influenced on an individual person. Therefore, the observed spectra of hairs along the hair filament are not the problem in unique identification of human hair.

The ATR FT-IR spectra of single hair acquired by the slide-on Ge IRE from different position on individual person were collected. The positions were divided into four parts and the three hair filaments were randomly analyzed for each

part at a, b, c, and d. The two hair filaments were randomly analyzed for each part as shown in Figure 4.9.

Figure 4.10 shows the observed spectra of hair from individual person with different position followed by Figure 4.9. The spectral features of hair at each different position on head of an individual person were the same because the different positions of hair on individual person has no considerable influence on hair structure and life style of person (i.e., ultraviolet (UV) irradiation, brushing, drying, heating, dietary, and healthy) factors. Although the different bands at 1042 and 1017  $\text{cm}^{-1}$  can be noticed, this band cannot be used for differentiating an individual person.



**Figure 4.8** Normalized ATR FT-IR spectra of hair were collected along the hair filament.



### The different positions of hairs on head

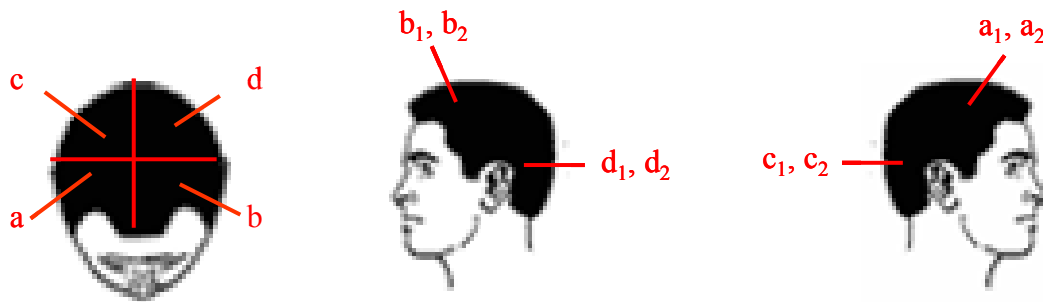


**Figure 4.9** Positions on individual person when hair sample were collected.

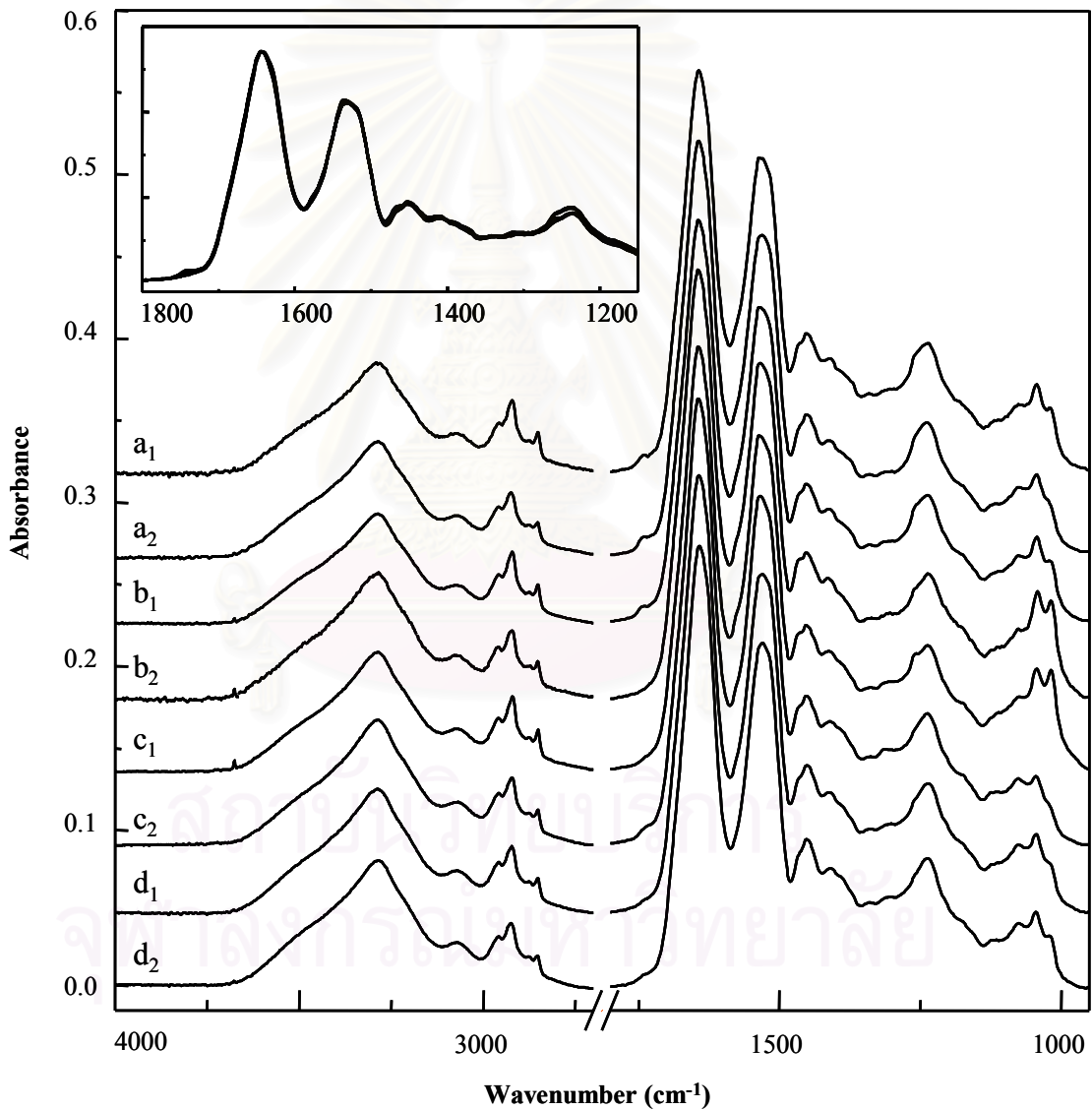


**Figure 4.10** Normalized spectra of hair acquired from the different positions of hair on head.

#### 4.3.1.5 ATR FT-IR Spectra of Hairs from Different Persons

This section was considerable the various position of hair filaments from individual person. The single human hair from the different age, gender, and natural hair color were collected by the homemade slide-on Ge  $\mu$ IRE. All spectra show the different spectral features as seen in Figure 4.11. Each spectrum shows the significant spectrum of absorption band of Amide I, II, and III. Because the individual person has a specific character of the protein structure and the factors of hair damage, the changing chemical structure were occurred. The different spectra of individual person can be used in unique identification of hair in forensic analysis. The absorption bands of range 1100-1000  $\text{cm}^{-1}$  show the different spectral intensity at 1042 and 1017  $\text{cm}^{-1}$  due to the interfering between the S=O stretching of protein structure of hair and Si-O-Si stretching of silicon oil being a composition of cosmetic

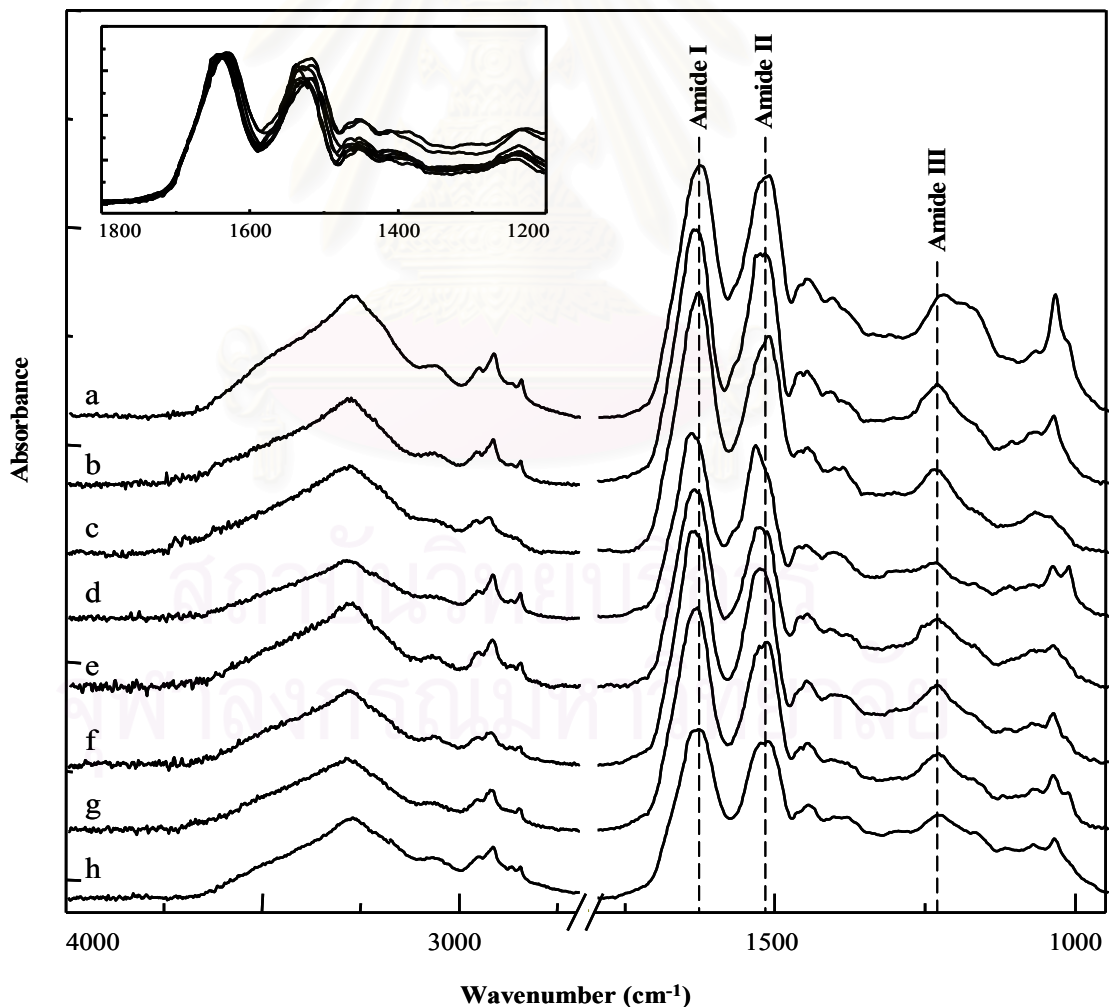


**Figure 4.11** Normalized spectra of single hair from different eight persons.

### 4.3.2 Chemical Treated-Hairs

Hair treatment includes hair coloring, hair permanent waving, hair bleaching, and hair straightening agents. These utilize fairly strong chemicals that are applied directly to the hair shaft, and the hair can be damaged. The hair damage was occurring by the breaking of protein bonds in hair. The chemical information of treated-human hair was changed in molecular level as shown in Figure 4.12.

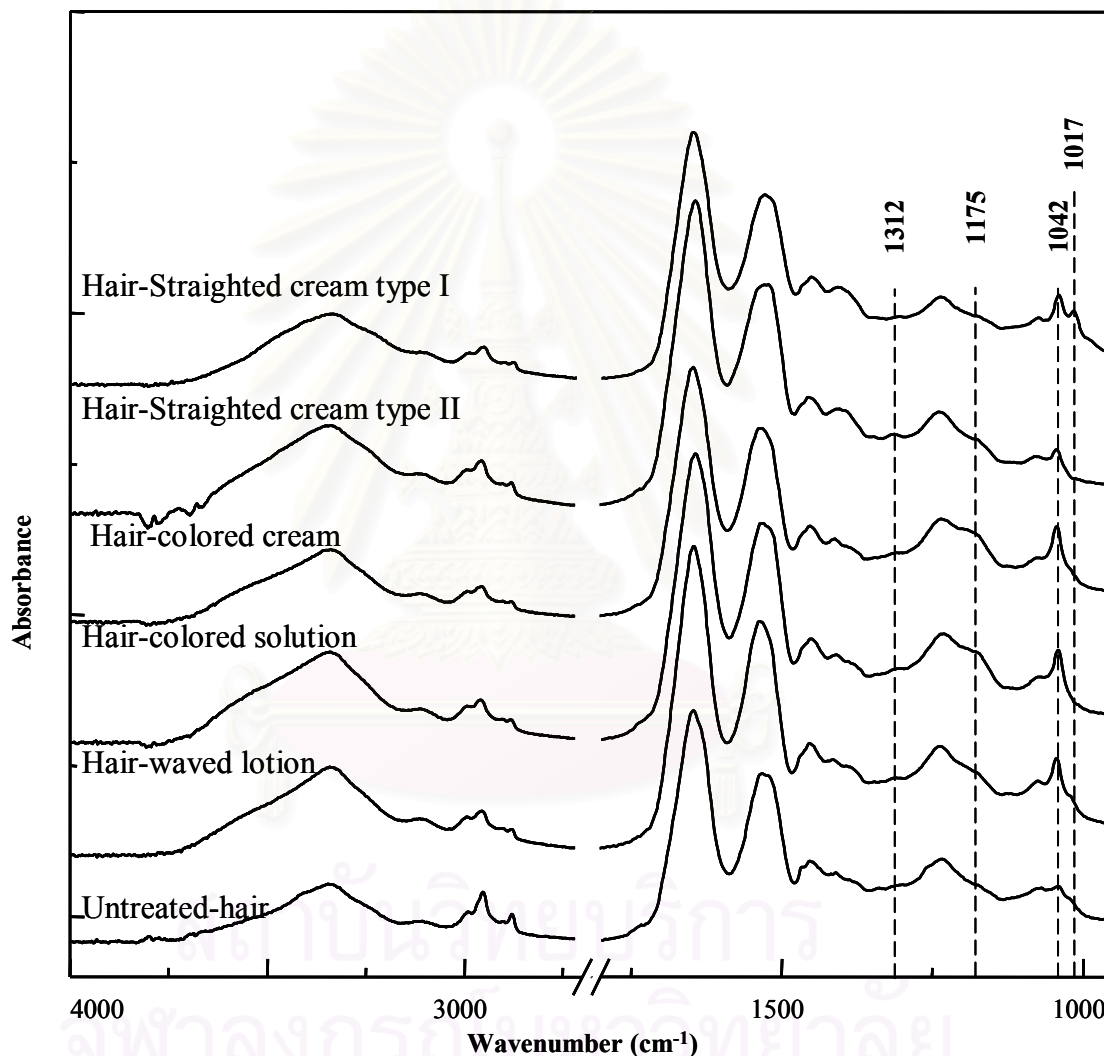


**Figure 4.12** ATR FT-IR spectra of treated single hair with different types of chemical treatment.

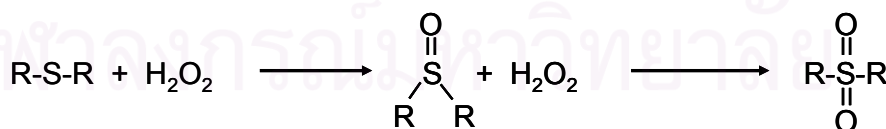
By comparison, the observed spectra of un-treated hair and chemical-treated hair with various types of treatment show the different spectral feature at Amide II. The absorption bands at 1042 and 1017 cm<sup>-1</sup> were increased because the increasing of S=O and Si-O-Si of hair treatment creams. The appearance of the absorption bands at 1312

and  $1175\text{ cm}^{-1}$  were assigned to the composition of hair treatment creams. Thus, the different chemical treatment of hair can identify the different treated-hair.

#### 4.3.2.1 ATR FT-IR Spectra of Hairs between Untreated-Hair and Straight Cream Treated-Hair

The main ingredient of permanent hair straightening chemicals is *thioglycolate* or *thio*. This chemical causes the breaking of the sulfur bonds of human hair before the hair taking a new shape. After that, the sulfur bond in hair was re-connected to form the new shape. The new shape of hair was used by the flattening or straightening irons.

The spectra of the untreated-human hair and the treatment with straight cream acquired by the homemade slide-on Ge  $\mu$ IRE are shown in Figure 4.13. The observed spectra of untreated-hair and straighted-hair were compared. The different peak shapes and peak positions at Amide II ( $1521$ ),  $1312$ ,  $1175$ , and  $1042\text{ cm}^{-1}$ , respectively, associated to the chemical information was changed in treated-hair. For the treated hair, the protein bond in hair was broken by the chemical ingredient of straight creams. The absorption bands of Amide II bands shifted to lower wavenumber due to the change of conformation of hair after treatment. In addition, the new absorption bands at  $1312$  and  $1175\text{ cm}^{-1}$  assigned to the composition of straight cream are also observed. The absorption band of S=O stretching at  $1042\text{ cm}^{-1}$  was increased. Due to the oxidation reaction of amino acid (cysteine) by hydrogen peroxide, the functional group of S=O in treated-hair was increased as follows:



From all obtained results ATR FT-IR spectra with ATR FT-IR technique can apply in forensic analysis (unique identification) and cosmetic analysis.

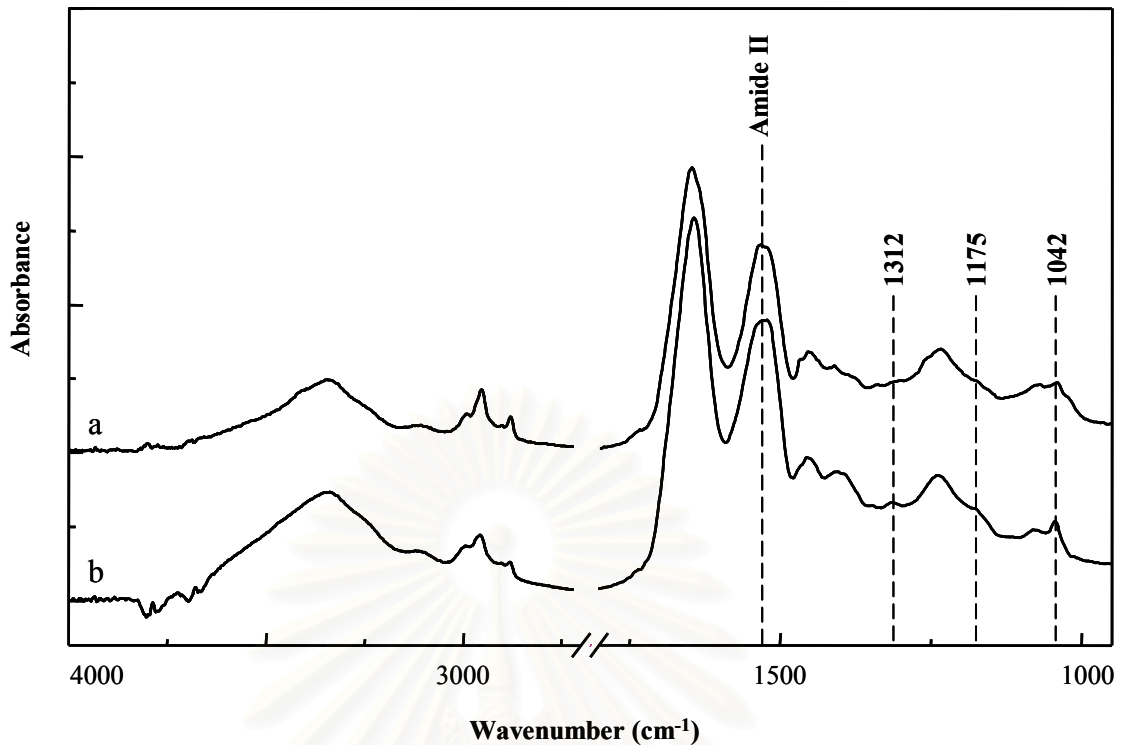


**Figure 4.13** ATR FT-IR spectra of hair (a) untreated-hair and (b) treated-hair with straight cream.

#### 4.3.2.2 ATR FT-IR Spectra of Hairs between Untreated-Hair and Permanent Wave Lotion Treated-Hair

The principle of permanent wavy process is the change of hair shape by using the chemical reagent such as reducing agent (usually ammonium thioglycolate) and oxidizing agent (hydrogen peroxide). The chemical reagent of permanent wave lotion damaged the protein bond (sulfur bond) and the cuticle layer of human hair. The new shape of hair can change by rollers or curlers and the sulfur bond will be re-connected.

Figure 4.14 shows the different spectra of untreated-hair and permanent wavy hair collected by the homemade slide-on Ge  $\mu$ IRE. Amide II band of treated-hair changing from  $\alpha$ -helix to  $\beta$ -sheet due to the chemical structure was changed in molecular level. Due to reforming the bond of alpha helices can shift position in relation to each amino acid composition by reducing agent. Also the broad band at  $1175\text{ cm}^{-1}$  related to the chemical reagent of cosmetic absorbing on the surface. The absorption band of S=O vibrational mode increasing at  $1042\text{ cm}^{-1}$  was assigned to

cysteic acid which occurred from the breaking of the sulfur bond of cystine in molecular level by chemical ingredient of permanent wave lotion.

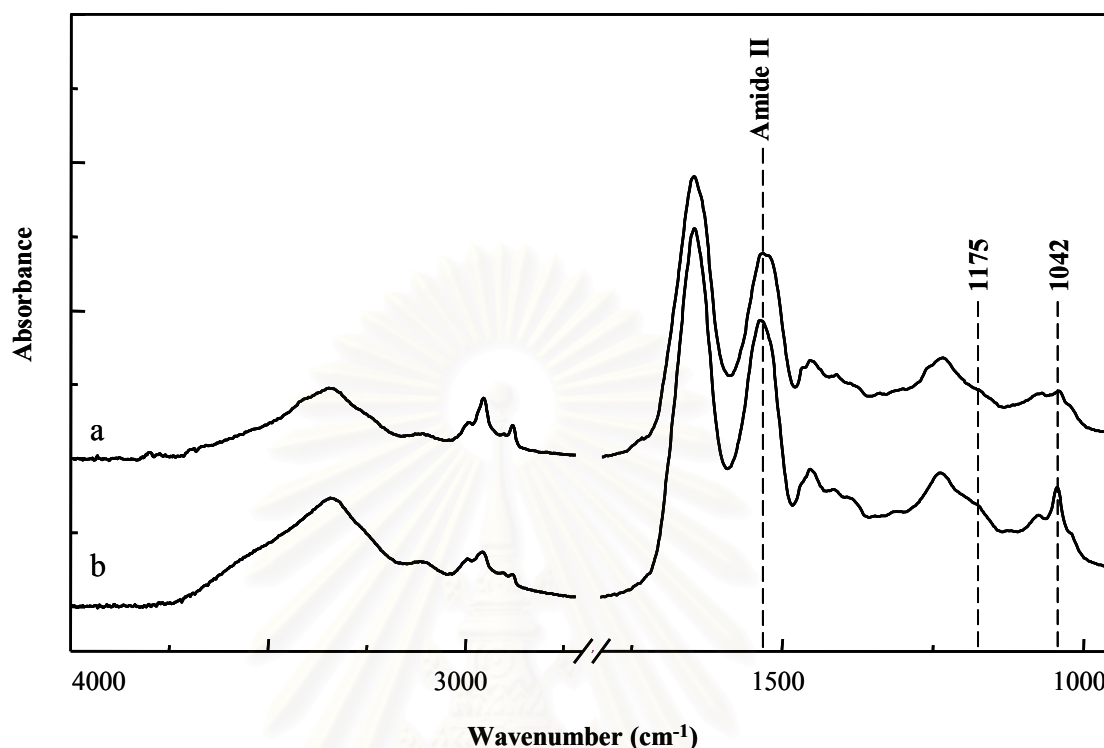


**Figure 4.14** ATR FT-IR spectra of hair (a) untreated-hair and (b) treated-hair with permanent wavy lotion.

#### 4.3.2.3 ATR FT-IR Spectra of Hairs between Untreated-Hair and Color Cream Treated-Hair

Hair coloring products consist of ammonia dyeing solution and hydrogen peroxide solution, which directly applied to the hair. The ammonia solution causes of the cracking of the cuticle layer of hair before the dye precursors are penetrated to this layer.

The change of chemical of human hair was induced by coloring have been previously reported [32, 50]. The study of the coloring effect was done by the homemade slide-on Ge  $\mu$ IRE accessory under the same experimental conditions for that of the untreated-hair. As seen in Figure 4.14b, the broad band at 1175 cm<sup>-1</sup> corresponding to the chemical in color cream on surface of hair was absorbed. Spectral intensity of symmetric stretching of S=O at 1042 cm<sup>-1</sup> was increased. The

peak shape of the Amide II band was changed because of the changing of hair structure by the interaction between the chemicals of color cream and protein bonds.

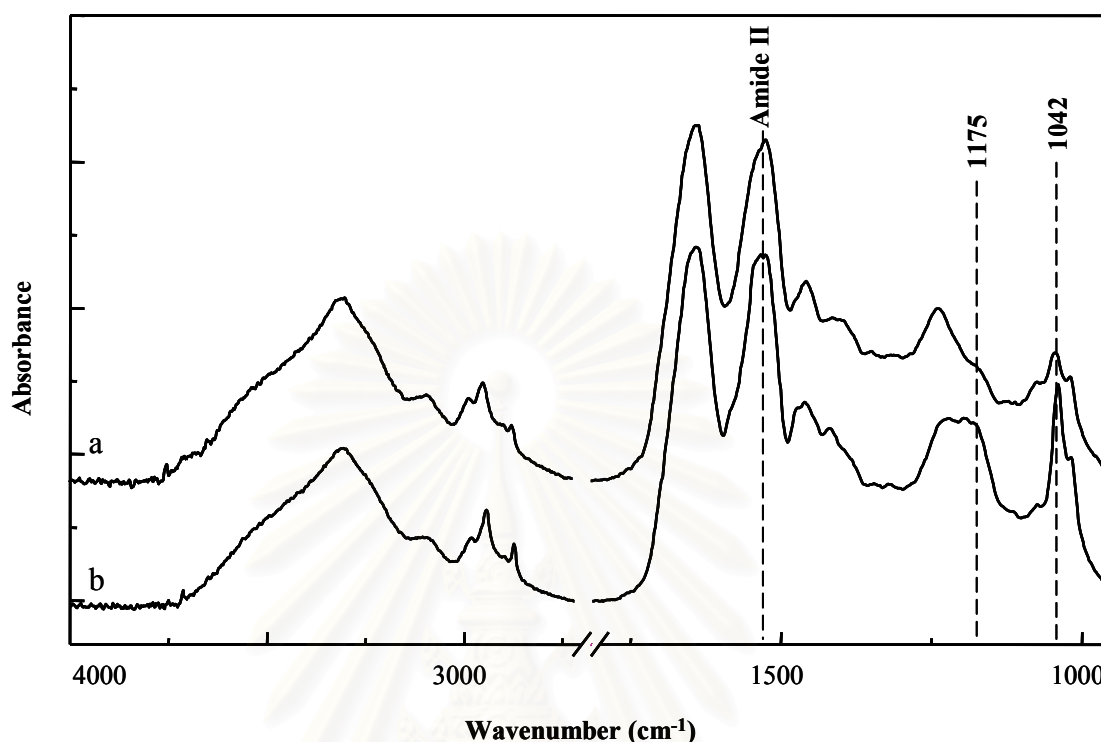


**Figure 4.15** ATR FT-IR spectra of hair (a) untreated-hair and (b) treated-hair with color cream.

ATR FT-IR microspectroscopy was successfully employed for spectral acquisitions of untreated-hair are different factors (i.e., age, gender, color, and person) and chemical treated-hair. This technique is non-destructive sample, without sample preparation and has a short analysis time and the results are reliable.

#### 4.4 Characterization of Trace Cosmetic on the Hairs Surface by using ATR FT-IR Spectroscopy

In the prior study, the different hair from person can be characterized by the homemade slide-on Ge  $\mu$ IRE. Characterization of trace cosmetic on hair surface is one part of the identifying of the different hair. Traditionally, the analysis of trace cosmetics or small amount of sample is difficult or cannot be analyzed due to the limitation of these techniques such as the small sample, destructive sample, required the sample preparation. This section shows the interesting of dominant and the



advantage of “*Contact-and-Collect*” technique for analysis of trace cosmetic on the hair surface by using the homemade slide-on Ge  $\mu$ IRE.

#### 4.4.1 Conventional ATR Technique

ATR FT-IR spectrum of clean hair by conventional ATR technique (Hemispherical Ge IRE) was shown in Figure 4.16A. After removing the hair from the IRE, the spectrum does not present the characteristic absorption band of residual cosmetic on the surface of the hair due to the contaminant was washed out several times with acetone. However, this spectrum of residue on IRE is not a straight line because of the effect of baseline correction. The ATR FT-IR spectra of uncleaned-hair show the different spectral features with the clean hair because the cosmetic was absorbed on surface and did not wash with acetone. The spectrum shows slightly weak spectral intensity absorption band at 1261, 1110, and 1016  $\text{cm}^{-1}$  which assigned to the cosmetic peaks on the surface of single human hair as shown in Figure 4.16B. This residual spectrum does not reveal the clearly characteristic band because sampling area of IRE has a large area comparing to the trace cosmetic on the hair surface and this technique required the alignment center between single hair and IRE. Thus, the conventional ATR technique is not suitable for the analysis of the trace cosmetic on the single hair.

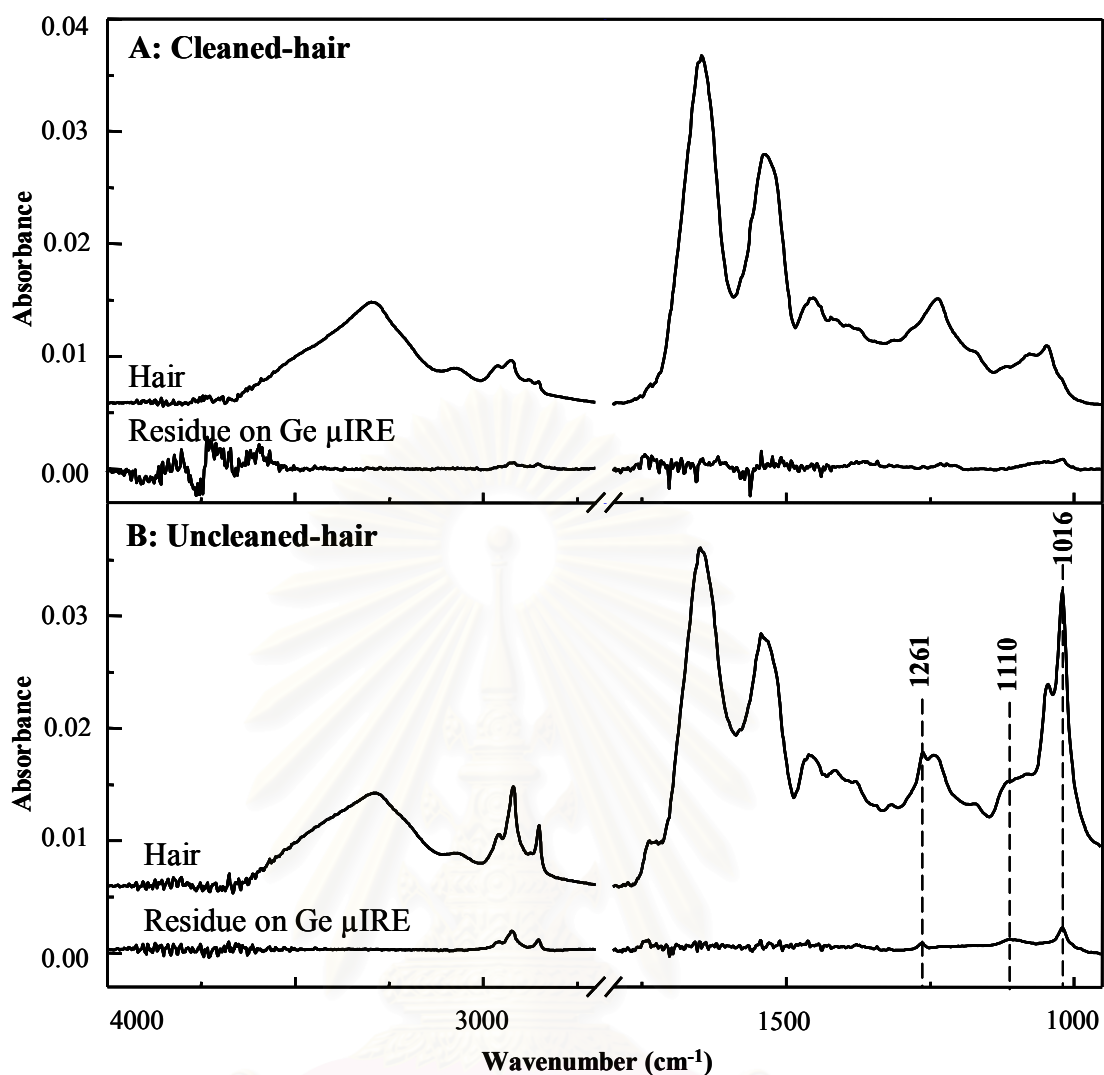


**Figure 4.16** ATR FT-IR spectra of hair and residual cosmetics on IRE (A) clean-hair and (B) uncleaned-hair acquired by the conventional ATR technique.

#### 4.4.2 Homemade Slide-on Ge $\mu$ ATR Technique

As previously described, the characterization of trace cosmetics by the conventional ATR technique was difficult for analysis. Thus, the analysis of trace cosmetic on surface from single human hair was developed by the homemade slide-on Ge  $\mu$ IRE. The novel technique called “*Contact-and-Collect*” –the measurement of trace cosmetics on the surface of single human hair (i.e., shampoos, hair conditioners and hair treatment cosmetics). When the tip of the Ge  $\mu$ IRE was brought into an optical contact with a single hair, some of the cosmetics on the hair surface were stuck

with the IRE. After removing the hair, the trace amount of the cosmetics on the IRE can be collected without any interference from hair. Figure 4.17A and B show the hair spectrum of clean hair, un-cleaned hair, and the residue of cosmetic on  $\mu$ IRE acquired by the slide-on Ge  $\mu$ IRE accessory.

The ATR FT-IR spectra of trace cosmetic on hair surface from two techniques – the homemade slide-on Ge  $\mu$ ATR and conventional ATR technique are compared. The homemade slide-on Ge  $\mu$ ATR technique gives the strong absorption band at 1048 and 1017  $\text{cm}^{-1}$  related to the silicone oil in cosmetic component. Spectral intensity of trace cosmetic is greater than that of trace cosmetic acquired by the conventional ATR technique. Since the homemade slide-on Ge  $\mu$ IRE has a small sample area, the selected position for analysis can be collected, and the amount of cosmetic can be increased by making several contacts before analysis. The clearly cosmetic spectra acquired by “*Contact-and-Collect*” technique can be simultaneously used the hair spectra for unique identification and forensic characterization of hair.

#### **4.4.2.1 Results of the Different Type of Cosmetics**

The spectra of different types cosmetic are shown in Figure 4.18. Each spectrum of hair using different type of cosmetic shows the unique spectra of each cosmetic because of their specific composition and ratio of the chemical reagents from different manufacture.

ATR FT-IR microspectroscopy is one of the powerful tools for a single human hair characterization and hair surface characterization. The observed spectra of single hair unique to the person show the specific difference of single hair depending on chemical structure of untreated-hair, chemical treated-hair, and cosmetics on hair surface. These highly specific differentiating spectra of single human can be employed for unique identification or for differentiation of hair based on the molecular structure of hairs and cosmetics on hairs.

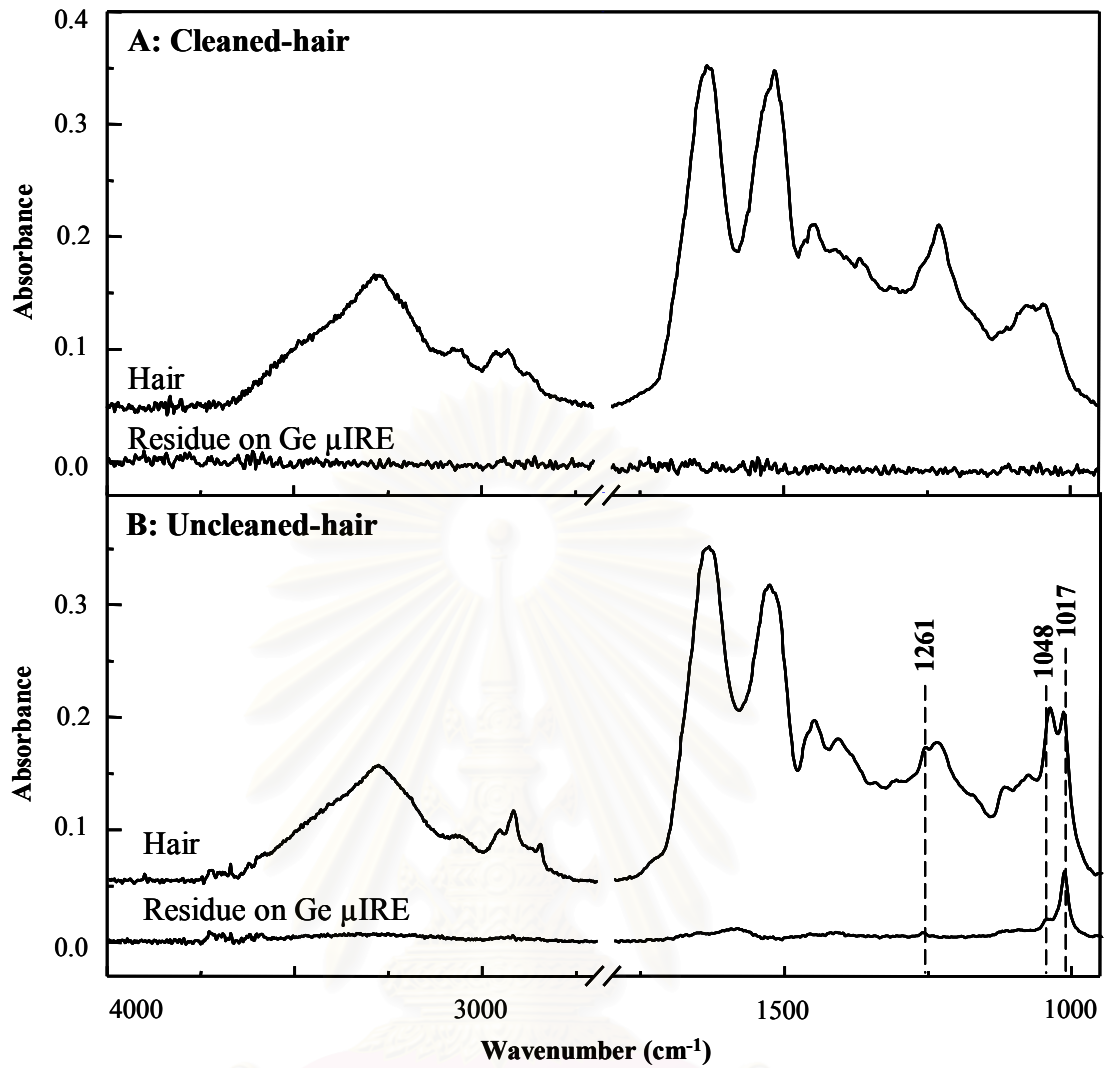


**Figure 4.17** ATR FT-IR spectra of hair and residual cosmetics on IRE (A) clean-hair and (B) uncleaned-hair acquired by the homemade slide-on Ge  $\mu$ IRE accessory.

สถาบันวิทยบริการ  
จุฬาลงกรณ์มหาวิทยาลัย

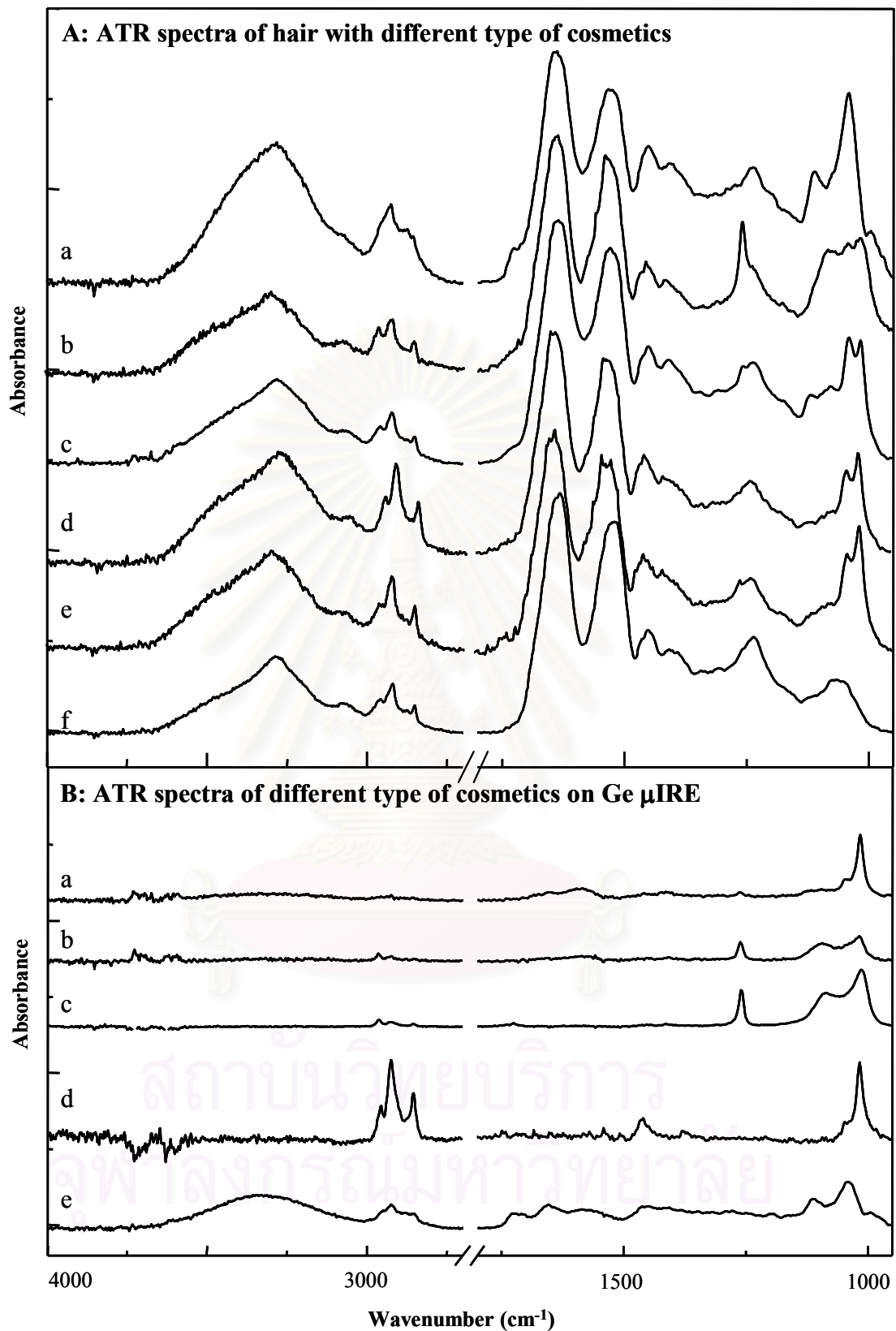


**Figure 4.18** ATR FT-IR spectra of hair and residual cosmetics on IRE: (A) hair and (B) residual cosmetics acquired by the homemade slide-on Ge  $\mu$ IRE accessory

#### 4.5 Characterization of Split Hairs by ATR FT-IR Microspectroscopy

Currently, the main problem of hair is the split hairs. The cause of this problem includes chemical treatment, physical wear, heat, and weather. To solve this problem - the study of changing chemical structure in split hairs was collected in this research.

Characterization of single split hairs by the homemade slide-on Ge  $\mu$ IRE is believed to associate with health and nature of the hair care of the person. ATR FT-IR spectra of the un-split hairs and split hair were shown in Figure 4.19. The spectra were acquired without an additional sample preparation. Spectral features of one filament (split hairs) were significantly different from the rest. The Amide I and Amide II bands showed a red shift, while a new peak was observed at  $1575\text{ cm}^{-1}$ . This band could be assigned to N-H scissoring vibration of  $\text{NH}_2$  occurring from the breaking of the peptide bond in protein structure of human hair. The observed phenomenon suggests that the splitting associated with the change of hair at the molecular level. The advantage of this procedure can be applied for prevention of the split hairs.

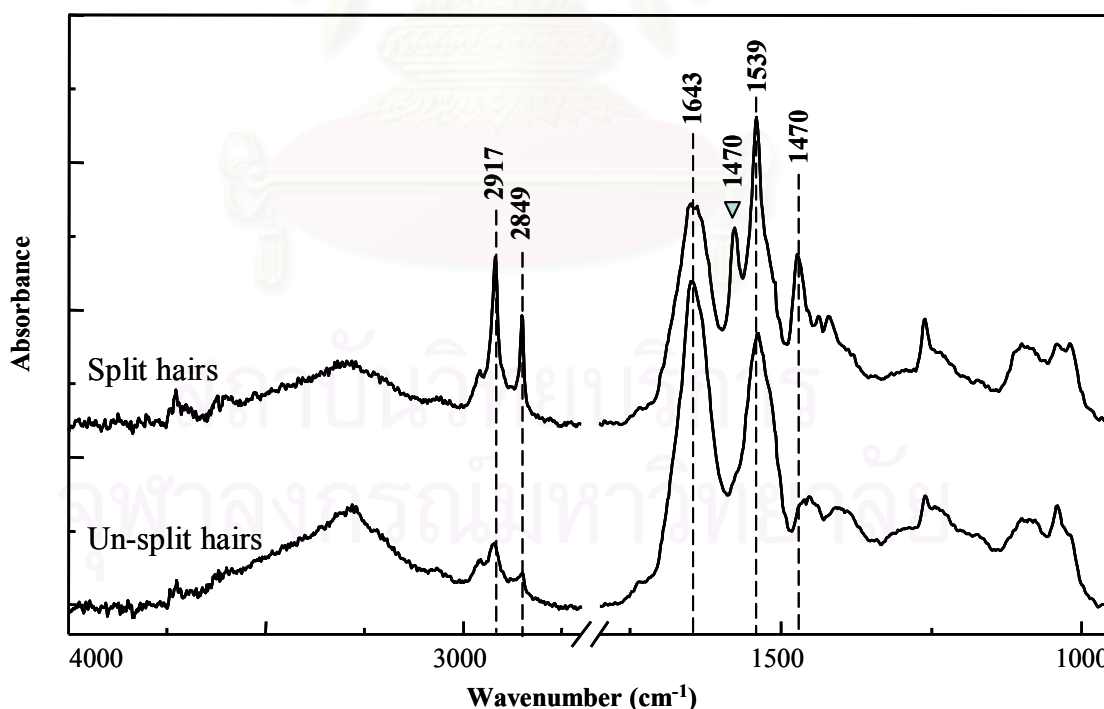


**Figure 4.19** ATR FT-IR spectra of split hairs and un-split hairs acquired by the homemade slide-on Ge  $\mu$ IRE accessory.

In order to ensure the measurement of the split hairs being associated to the change of hair at the molecular level, ATR FT-IR spectra of un-split hairs, split hairs and making-split hairs were collected as shown in Figure 4.20.

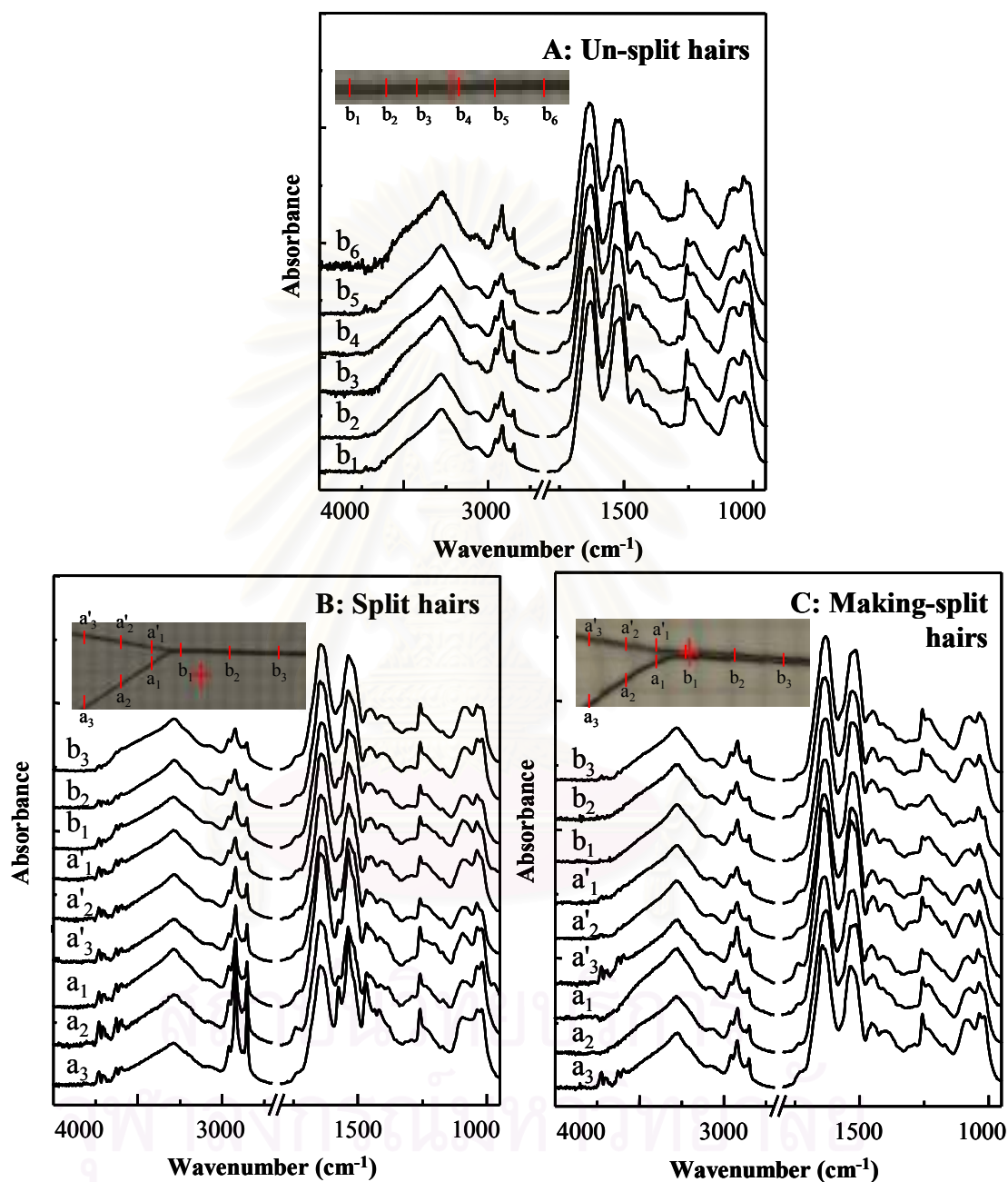


**Figure 4.20** ATR FT-IR spectra of hair acquired by the homemade slide-on Ge  $\mu$ IRE: (A) Un-split hairs, (B) Split hairs, and (C) Making-split hairs.

The observed spectra of un-split hairs and making-split hairs show the same spectral features of Amide I and Amide II. The observed spectra of split hairs showed



the new peak at  $1575\text{ cm}^{-1}$  and the absorption bands of Amide I and Amide II showed a red shift, as mentioned before. Thus new peak found at  $1575\text{ cm}^{-1}$  in the split hairs associated to the change of hair at the molecular level [51].

In this section, ATR FT-IR spectra of split hair acquired by the slide-on Ge IRE can be analyzed for differentiation between un-split hair and split hair, and natural split hair and making-split hair based on the change of the molecular level of hair structure, and this technique can be applied to biological analysis, forensic analysis, and cosmetic industrial analysis.



สถาบันวิทยบริการ  
จุฬาลงกรณ์มหาวิทยาลัย

## CHAPTER V

### CONCLUSIONS

ATR FT-IR microspectroscopy is suitable for analysis of single human hair. Experimental procedure is easy without additional sample preparations, non-destruction technique and short analysis time and the results are reliable. The ATR FT-IR spectrum gives the chemical information associated with the molecular structure of human hair. The spectral quality of hair spectra acquired by Ge  $\mu$ IRE is greater than that of conventional ATR technique.

The homemade slide-on Ge  $\mu$ IRE accessory has a small sampling area (less than  $100 \times 100 \mu\text{m}^2$ ). This accessory was successfully employed for investigating the small sample such as single human hair. For the characterization of human hair by ATR FT-IR microspectroscopy; this method can identify the chemical structure and differentiate the types of the cosmetic on the surface of the human hairs by the novel technique called "*Contact and Collect*". Regarding to the ATR spectra of human hairs, the observed spectra show the different spectral features from different persons and the difference between un-split and split hairs. In the same person, the observed spectra show the same spectral type from different position according to the unique characteristic of hairs from individual person. It is concluded that the homemade slide-on Ge  $\mu$ IRE accessory can be applied for forensic analysis of hair.

#### **Suggestion for future work**

The homemade slide-on Ge  $\mu$ IRE accessory and the "*Contact and Collect*" technique show the high efficiency for analysis of single human hair and cosmetic on surface of single human hair which have a small sample and small amount of sample, respectively. This accessory and this technique are probably employed for forensic analysis of human hair in real case.

Moreover, the homemade slide-on Ge  $\mu$ IRE accessory can be used in many applications to perform with various samples for advanced analysis such as the forensic analysis, cosmetic industries, food packaging, textile technology, and polymer industries due to the small sample area, non-destructive sample, without sample preparation, and short analysis time.



สถาบันวิทยบริการ  
จุฬาลงกรณ์มหาวิทยาลัย

## REFERENCES

- [1] Akhtar, W.; Edwards, H.G.M.; Farwell, D.W.; and Nutbrown, M. Fourier-Transform Raman Spectroscopy Study of Human Hair. Spectro. Acta Pt. A. 53 (1997): 1021-1031.
- [2] Gaillard, Y.; and Pépin, G. Screening and Identification of Drug in Human Hair by High-Performance Liquid Chromatography-Photodiode-Array UV Detection and Gas Chromatography-Mass Spectrometry After Solid-Phase Extraction A Powerful in Forensic Medicine. J. Chromatogr. A. 762 (1997): 251-267.
- [3] Nakashima, K. High-Performance Liquid Chromatographic Analysis of Drug of Abuse in Biologic Samples. J. Health Sci. 51 (2005): 272-277.
- [4] Phinney, K.W.; and Sander, L.C. Liquid Chromatographic Method for the Determination of Enantiomeric Composition of Amphetamine and Methamphetamine in Hair Samples. Anal. Bioanal. Chem. 378 (2004): 144–149.
- [5] Villain, M.; Concheiro, M.; Cirimele, V.; and Kintz, P. Screening Method for Benzodiazepines and Hypnotics in Hair at pg/mg Level by Liquid Chromatography–Mass Spectrometry/mass Spectrometry. J. Chromatogr. B. 825 (2005): 72–78.
- [6] Felli, M.; Martello, S.; Marsili, R.; and Chiarotti, M. Disappearance of Cocaine from Human Hair after Abstinence. Forensic Sci. Int. 154 (2005): 96–98.
- [7] Beránková, K.; Habrdová, V.; Balíková M.; and Strejc, P. Methamphetamine in Hair and Interpretation of Forensic Findings in a Fatal Case. Forensic Sci. Int. 153 (2005): 93–97.
- [8] Kintz, R.; Cirimele, V.; Edel, Y.; Tracqui, A.; and Mangin, P. Characterization of Dextromoramide (Palfium) Abuse by Hair Analysis in a Denied Case. Int. J. Leg Med. 107 (1995): 269-272.

- [9] Lachenmeier, K.; Musshoff, F.; and Madea, B. Determination of Opiates and Cocaine in Hair using Automated Enzyme Immunoassay Screening Methodologies followed by Gas Chromatographic–Mass Spectrometric (GC–MS) Confirmation. Forensic Sci. Int. 159 (2006): 189–199.
- [10] Han, E.; Park, Y.; Yang, W.; Lee, J.; Lee, S.; Kim, E.; Lim, M.; and Chung, H. The Study of Metabolite-to-Parent Drug Ratios of Methamphetamine and Methylenedioxymethamphetamine in Hair. Forensic Sci. Int. 161 (2006): 124–129.
- [11] Nishida, M.; Yashiki, M.; Namera, A.; and Kimura, K. Single Hair Analysis of Methamphetamine and Amphetamine by Solid Phase Microextraction Coupled with in Matrix Derivatization. J. Chromatogr. B. 842 (2006): 106–110.
- [12] Munakata, M.; Onuma, A.; Kobayashi, Y.; Haginoya, K.; Yokoyama, H.; Fujiwara, I.; Yasuda, H.; Tsutsui, T.; and Inuma, K. A Preliminary Analysis of Trace Elements in the Scalp Hair of Patients with Severe Motor Disabilities Receiving Enteral Nutrition. Brain Dev. 28 (2006): 521–525.
- [13] Chen, B.J.; Lee, P.L.; Chen, W.Y.; Mai, F.D.; and Ling, Y.C. Hair Dye Distribution in Human Hair by ToF-SIMS. Appl. Surf. Sci. 252 (2006): 6786–6788.
- [14] Kempson, I.M.; Skinner, W.M.; and Kirkbride, P.K. Calcium Distributions in Human Hair by ToF-SIMS. Biochim. Biophys. Acta. 1624 (2003): 1–5.
- [15] Kuzuhara, A.; and Hori, T. Reduction Mechanism of Triglycolic Acid on Keratin Fibers using Microspectrophotometry and FT-Raman Spectroscopy. Polymer. 44 (2003): 7963-7970.
- [16] Salas, A.M.; Lareu, V.; and Carracedo, A. Heteroplasmy in mtDNA and the Weight of Evidence in Forensic mtDNA Analysis: A Case Report. Int. J. Legal Med. 114 (2001):186–190.
- [17] Wang, Q.; and Boles, R.G. Individual Human Hair Mitochondrial DNA Control Region Heteroplasmy Proportions in Mothers and Children. Mitochondrion. 6 (2006): 37–42.

- [18] Amendt, Jens.; Krettek, R.; and Zehner, R. Forensic Entomology. Naturwissenschaften. 91 (2004): 51–65.
- [19] Kintz, P.; Tracqui, A.; and Mangin, P. Detection of Drugs in Human Hair for Clinical and Forensic Applications. Int. J. Leg Med. 105 (1992): 1-4.
- [20] Brettell, T.A.; Inman, K.; Rudin, N.; and Saferstein, R. Forensic Science. Anal. Chem. 73 (2001): 2735-2744.
- [21] Srogi, K. Testing for Drugs in Hair-A Review of Chromatographic Procedures. Microchim. Acta. 154 (2006): 191-212.
- [22] Chojnacka, K.; Górecka, H.; and Górecki, H. The Effect of Age, Sex, Smoking Habit, and Hair Color on the Composition of Hair. Environ. Toxicol. Pharmacol. 22 (2006): 52-57.
- [23] Brewer, W.E.; Galipo, R.C.; Sellers, K.W.; and Morgan, S.L. Analysis of Cocaine, Benzoyllecgonine, Codeine, and Morphine in Hair by Supercritical Fluid Extraction with Carbon Dioxide Modified with Methanol. Anal. Chem. 73 (2001): 2371-2367.
- [24] Kempson, I.M.; and Skinner, W.M. Advanced Analysis of Metal Distributions in Human Hair. Environ. Sci. Technol. 40 (2006): 3423-3428.
- [25] Scheidweiler, K.B.; and Huestis, M.A. Simultaneous Quantification of Opiates, Cocaine, and Metabolites in Hair by LC-APCI-MS/MS. Anal. Chem. 76 (2004): 4358-4363.
- [26] Wada, M.; and Nakashima, K. Hair Analysis: An Excellent Tool for Confirmation of Drug Abuse. Anal. Bioanal. Chem. 385 (2006): 413-415.
- [27] Mieczkowski, T.; and Kruger, M. Interpreting the Color Effect of Melanin on Cocaine and Benzoyllecgonine Assays for Hair Analysis: Brown and Black Samples Compared. J. Clin. Forensic Med. 14 (2007): 7-15.
- [28] Turesky, R.J.; Freeman, J.P.; Holland, R.D.; Nestorick, D.M.; Miller, D.W.; Ratnasinghe, D.L.; and Kadlubar, F.F. Identification of Aminobiphenyl Derivatives in Commercial Hair Dyes. Chem. Res. Toxicol. 16 (2003): 1162-1173.
- [29] Hartwig, S.; Auwärter, V.; and Pragst, F. Effect of Hair Care and Cosmetics on the Concentrations of Fatty Acid Ethyl Esters in Hair as Markers of Chronically Elevated Alcohol Consumption. Forensic Sci. Int. 131 (2003): 90-97.



- [30] Motz-Schalck, L.; and Lemaire, J. Photochemical and Thermal Modifications of Permanent Hair Dyes. J. Photochem. Photobiol. A-Chem. 147 (2002): 225–231.
- [31] Smith, B.C. Fundamentals of Fourier Transform Infrared Spectroscopy. New York: CRC Press, 1996.
- [32] Panayiotou, H.; and Kokot, S. Matching and Discrimination of Single Human-Scalp Hairs by FT-IR Micro-Spectroscopy and Chemometrics. Anal. Chim. Acta. 392 (1999): 223-235.
- [33] Bilińska, B. On the Structure of Human Hair Melanins from an Infrared Spectroscopy Analysis of their Interactions with  $\text{Cu}^{2+}$  Ions. Spectrochim. Acta Pt. A. 57 (2001): 2525–2533.
- [34] Feughelman, M.; Lyman, D.J. and Willis, B.K. The Parallel Helices of the Intermediate Filaments of  $\alpha$ -keratin. Int. J. Biol. Macromol. 30 (2002): 95–96
- [35] Wilk, K.E.; James, V.J.; and Amemiya, Y. The Intermediate Filament Structure of Human Hair. Biochim. Biophys. Acta. 1245 (1995): 392-396.
- [36] Nестea, D.V.; and Tobin, D.J. Hair Cycle and Hair Pigmentation: Dynamic Interactions and Changes Associated with Aging. Micron. 35 (2004): 193–200.
- [37] Pragst, F.; and Balikova, M.A. State of the Art in Hair Analysis for Detection of Drug and Alcohol Abuse. Clin. Chim. Acta. 370 (2006): 17–49.
- [38] Kajiura, Y.; Watanabe, S.; Itou, T.; Nakamura, K.; Iida, A.; Inoue, K.; Yagi, N.; Shinohara, Y.; and Amemiya, Y. Structural Analysis of Human Hair Single Fibres by Scanning Microbeam SAXS. J. Struct. Biol. 155 (2006): 438–444.
- [39] Robbins, C.R.; and Kelly, C.H. Amino Acid Composition of Human Hair. Text. Res. J. 40 (1970): 891-896.
- [40] Johnson, R.J.; Wiersema, V.; and Kraft, I.A. Hair Amino Acids in Childhood Autism. J. Autism Child. Schizophre. 4 (1974): 187-188.
- [41] Uran, M.W. Attenuated Total Reflectance Spectroscopy of Polymers Theory and Practice. Washington, DC: American Chemical Society, 1996.
- [42] Mirabella, F.M. Internal Reflection Spectroscopy Theory and Applications. New York: Marcel Dekker, 1993.



- [43] Chalmers, J.M.; and Griffiths, P.R. Hand Book of Vibrational Spectroscopy. Chichester: John Wiley & Sons, 2002.
- [44] Ekgasit, S.; and Padermshoke, A. Optical Contact in ATR/FT-IR Spectroscopy. Appl. Spectrosc. 55 (2001): 1352-1359.
- [45] Bower, D.I.; and Maddams, W.F. The Vibrational Spectroscopy of Polymers. New York: Cambridge University Press, 1989.
- [46] Workman, J., Jr.; and Springsteen, A.W. Applied Spectroscopy A Compact Reference for Practitioners. New York: Academic Press, 1998.
- [47] Lyman, D.J.; and Murray-Wijelath, J. Fourier Transform Infrared Attenuated Total Reflection Analysis of Human Hair: Comparison of Hair from Breast Cancer Patients with Hair from Healthy Subjects. Appl. Spectrosc. 59 (2005): 26-32.
- [48] Walsh, G. Proteins Biochemistry and Biotechnology. Chichester: John Wiley & Sons, 2002.
- [49] Nishikawa, N.; Tanizawa, Y.; Shoichi, T.; Horiguchi, Y.; and Asakura, T. Structural Change of Keratin Pprotein in Human Hair by Permanent Waving Treatment. Polymer. 39 (1998): 3835-3840.
- [50] Scanavez, C.; Silveira, M.; and Joekes, I. Human Hair: Color Changes Caused by Daily Care Damages on Ultra-structure. Colloid Surf. B-Biointerfaces. 28 (2003): 39-52.
- [51] Bellamy, L.J. The Infra-red Spectra of Complex Molecules. New York: John Wiley & Sons, 1958.
- [52] Socrates, G. Infrared and Raman Characteristic Group Frequencies Table and Charts. Chichester: John Wiley & Sons, 2001.
- [53] Colthup, N.B.; Daly, L.H.; and Wiberley, S.E. Introduction to Infrared and Raman Spectroscopy. New York: Academic Press, 1990.

# CURRICULUM VITAE

Suwimol Naranitad

- 1983      Born:      April, 12<sup>nd</sup>, in Bangkok, Thailand  
            Father:    Mr. Boonkuea Naranitad  
            Mother:    Mrs. Amporn Naranitad
- 1994      Primary School,  
            Nakornpathom Kindergarten, Nakornpathom
- 2000      High School,  
            Princess Sirindhorn's College, Nakornpathom
- 2004      Bachelor of Science (Chemistry),  
            Suan Dusit Rajabhat University, Bangkok, Thailand
- 2006      Master of Science (Petrochemistry and Polymer Science),  
            Chulalongkorn University, Bangkok, Thailand

สถาบันวิทยบริการ  
จุฬาลงกรณ์มหาวิทยาลัย